COMPUTATIONAL MECHANISTIC STUDIES OF THE DEAROMATIVE INTRAMOLECULAR DI-DEHYDRO DIELS-ALDER (IMDDA) REACTIONS OF ENE-YNE SUBSTITUTED HETEROARENES

by

Elena Kusevska

BSc. Applied Chemistry, Ss. Cyril and Methoudious University, 2013

MSc. European Master in Theoretical Chemistry and Computational Modeling, Autonomous University of Madrid, 2015

Submitted to the Graduate Faculty of the

Dietrich School of Arts and Sciences in partial fulfillment

of the requirements for the degree of

Master of Science

University of Pittsburgh

2019

UNIVERSITY OF PITTSBURGH

DIETRICH SCHOOS OF ARTS AND SCIENCES

This thesis was presented

by

Elena Kusevska

It was defended on

May 8th, 2019

and approved by

Peng Liu, Assistant Professor, Department of Chemistry

Kay M. Brummond, Professor, Department of Chemistry

Kenneth D. Jordan, Professor, Department of Chemistry

J. Karl Johnson, Professor, Department of Chemical and Petroleum Engineering

COMPUTATIONAL MECHANISTIC STUDIES OF THE DEAROMATIVE INTRAMOLECULAR DI-DEHYDRO DIELS-ALDER (IMDDA) REACTIONS OF ENE-YNE SUBSTITUTED HETEROARENES

Elena Kusevska, MS

University of Pittsburgh, 2019

I have carried out density functional theory calculations on the IMMDA reactions of a series of ene-yne substituted heteroarenes, in order to understand the effects of the identity and position of substitution of the tether, the identity of the diene heteroarene, and the presence of an additional benzene ring fused to the diene heteroarene, on the mechanism and selectivity of the intramolecular Diels-Alder (DA) reaction. For a subset of these reactions, I have compared the computed free energies of reaction, the free energies of activation, and the gas phase bond-dissociation energies and acidities of DA adducts with the experimentally determined activation free energies and reaction selectivities for the final product. The results indicate that the mechanism of the DA step involves several competing pathways, including the concerted cycloadditions and the stepwise additions with either the s-cis or s-trans conformers of the ene-yne substrates. The computational studies also suggest that the product selectivity of the IMDDA reaction is under kinetic control, and that the isomerized cyclohexadiene product is most likely formed through an ionic mechanism

TABLE OF CONTENTS

LIST OF TABLES

LIST OF FIGURES

1.0 INTRODUCTION

Intramolecular dehydro Diels-Alder (IMDDA) reactions[1-8] are widely used in organic synthesis for the formation of polycyclic, aromatic, and heteroaromatic compounds. They are furthermore interesting to study for theoretical reasons, because they can exhibit reaction mechanisms that are different from what has been observed for traditional Diels-Alder (DA) reactions. This thesis is an attempt to provide a greater understanding of the reactivity and selectivity of the intramolecular di-dehydro Diels-Alder reactions of a set of 2- and 3- ene-yne substituted heteroaromatic dienes. The main focus of this study is on understanding the effect of the position of substitution and the identity of the tether, the effect of an additional benzene ring fused to the heteroarene diene, and the effect of the identity of the heteroatom. I have performed a series of DFT calculations in order to understand the way in which these factors influence the mechanism of the DA cycloaddition and the selectivity for the final products in the IMDDA reaction. Further insight was obtained by comparing my computational results with the results of experimental studies that have been carried out in the group of Dr. Kay M. Brummond.

1.1 MECHANISM OF THE DIELS-ALDER REACTION

The traditional Diels-Alder reaction is a [4+2] intermolecular cycloaddition between a diene and a dienophile. It was first described by Otto Diels and Kurt Alder in 1928[9], and it has since become one of the most well-known methods in organic synthesis for the generation of six-membered (cyclohexene) rings[10-11]. In the Diels-Alder reaction, three C-C π-bonds are broken, and two C-C σ-bonds and one new C-C π-bond are formed. As a result this is an exothermic process during which up to 4 sp^2 carbons are converted into sp^3 stereocenters.

The Diels-Alder reaction is one of the most studied reactions in organic chemistry, and it is still relevant today. This is not surprising. It offers a straightforward method (the traditional DA reaction doesn't require a catalyst, few intermediates are produced, and the reaction conditions can be relatively mild) for the formation of six-membered rings[12-14] that are ubiquitous among biological and biologically-active products, as well as a variety of materials in electronics, and in polymers. It is furthermore a model reaction through which various theoretical and computational approaches for the study of chemical reactions have been developed and popularized. For example, the utility of molecular orbitals in the study of organic reactions became apparent through the theory of symmetry-based orbital correlation developed by Woodward and Hoffman[15-16] and the frontier molecular orbital (FMO) theory developed by Fukui[17-18]. Other examples are the study of transition state aromaticity by Zimmerman[19], the distortion-interaction

model developed by Houk[20], and most recently, the application of molecular dynamics (MD) simulations to the study of chemical systems with more complex reaction dynamics than can be described by traditional transition state theory (TST)[21-23]. The Diels-Alder reaction is a good model for theoretical investigation because it provides us with chemical systems that are simple enough, while at the same time offering a significant amount of diversity by varying the substitution pattern.

Two main mechanistic pathways, a concerted and a stepwise one, are known for the standard DA reaction. We can illustrate these by considering the simplest case of a DA reaction, that between 1,3-butadiene and ethylene shown in Figure 1. In both the concerted and stepwise case, butadiene can approach ethylene either in the s-cis conformation (1), or in the s-trans conformation (5), which is more stable by 3.5 kcal/mol at the B3LYP/6-31G* level of theory[24]. This means that both an s-cis and an s-trans concerted mechanism, and an s-cis and an s-trans stepwise mechanism are conceivable.

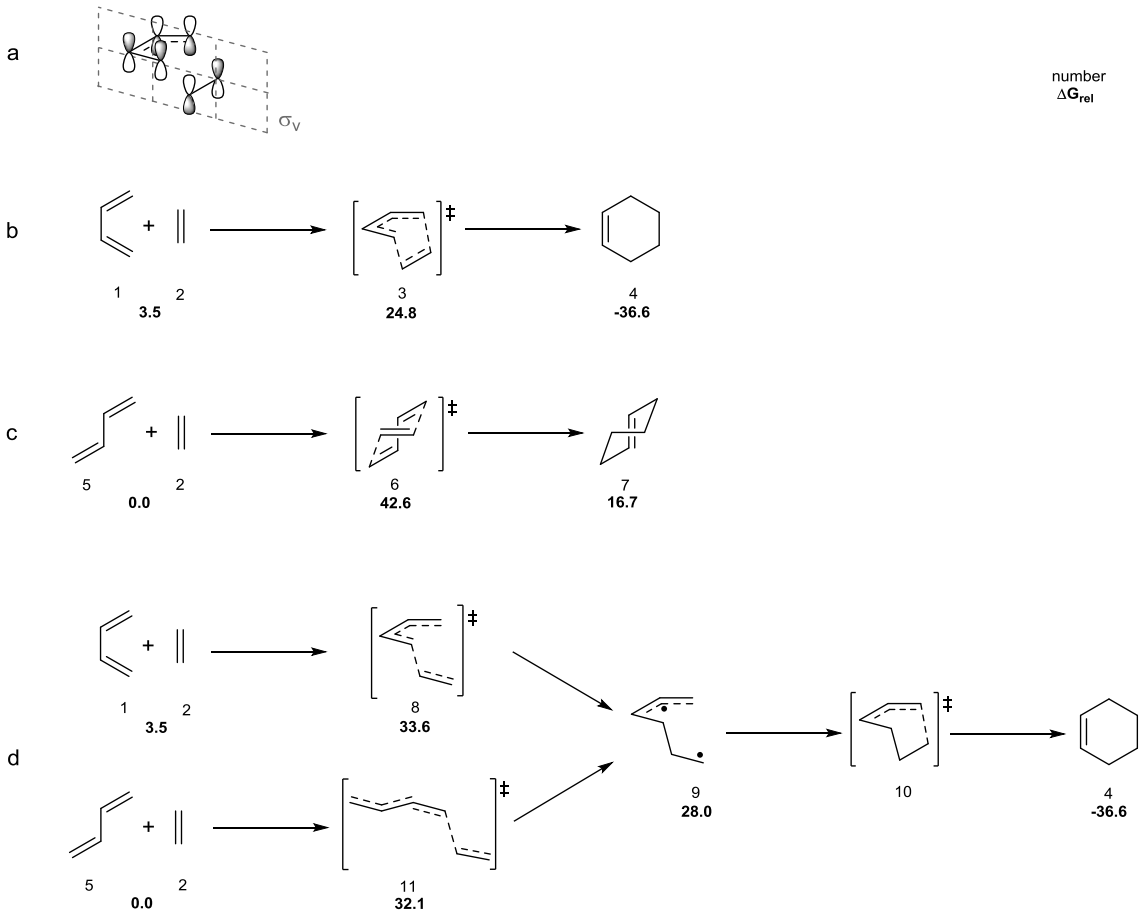

Figure 1 The DA reaction between 1,3-butadiene and etylene. a) A plane of symmetry is conserved for the concerted mechanism b) The concerted reaction mechanism with 1,3-butadiene in the s-cis conformation, passing through the pericyclic transition state (3) c) The concerted reaction mechanism with 1,3-butadiene in the s-trans conformation d) the stepwise mechanism, passing through a diradical stepwise transition state (8 and 11) and a diradical intermediate (9). The reported values are electronic energies calculated at the (U)B3LYP/6-31G level of theory, taken from references 21 and 24.*

It has long been established from the results of both experimental and computational studies that for the Diels-Alder reaction between ethylene and 1,3-butadiene, the concerted mechanism with 1,3-butadiene maintained in the s-cis conformation throughout the course of the reaction (Figure 1b) is preferred[24-28]. This is because the s-cis concerted mechanism is the most electronically favorable one.

Apart from the more recent computational studies, the electronic structure of the s-cis concerted mechanism has also been studied in the past in the above referenced classic theoretical papers by Woodward and Hoffman, Fukui, and Zimmerman. These theoretical studies established that the s-cis concerted mechanism is an electronically favorable thermally allowed process that proceeds via a synchronous pericyclic transition state (3). For example, looking at Figure 1a, we can see that in the normal electron demand DA reaction, the HOMO of ethylene and the LUMO of butadiene are both antisymmetric with respect to the plane of symmetry, σ_v. In addition to this, the HOMO and LUMO are also in phase on the carbons where the new σ-bonds are formed. Fukui argued that because of this, the frontier molecular orbitals on the ethylene and butadiene will have a constructive interaction, making the reaction electronically favorable.

Furthermore, we can see that for the approach of reactants shown in Figure 1a, σ_v is conserved throughout the reaction. Woodward and Hoffman showed that in this case the molecular orbitals in the reactant and the product are correlated, in the sense that, during the course of the reaction, molecular orbitals of a given symmetry with respect to σ_v in the approaching reactants will be transformed into orbitals of the same symmetry in the resulting product. Because all the occupied molecular orbitals of the product are correlated through symmetry with those in the reactants, the ground state of the product correlates with the ground state of the reactants and as a result, the reaction is thermally allowed. Thermal energy from collisions is enough to allow the reactants to overcome the energy barrier associated with the changes in electronic energy and proceed to products. Although seemingly qualitative, this result is exact because populated MOs correspond to electronic states, and electronic states of a given symmetry in the reactant correlate with electronic states of the same symmetry in the product.

In addition to all this, another factor that contributes to the electronic favorability of the concerted pericyclic s-cis transition state is the fact that the pericyclic [4+2] transition state is a Hückel system with 6 electrons, so it is stabilized by aromaticity.

Conversely, if the diene was instead maintained in the s-trans conformation throughout the reaction coordinate (Figure 1c), a symmetry element (C_2) would still be conserved[29], but the s-trans concerted transition state (6) is much higher in energy than the s-cis concerted transition state (3) and the final product of this reaction is the much more unstable trans-cyclohexene (7) rather than cis-cyclohexene (4). The reason for the lower stability of both 6 and 7, is that in both cases there is a pyramidal geometry enforced on the sp^2 carbons of the π-bond in the highly strained geometry of the molecule.[24, 29-30] As a result of all this, the s-trans concerted transition state is much less favorable than the s-cis concerted transition state, the s-trans concerted cycloaddition reaction is endothermic rather than exothermic, and as a consequence, this mechanism is very unlikely.

Turning our attention to the stepwise mechanisms shown in Figure 1d, we can see that for the case of a DA reaction between ethylene and 1,3-butadiene in the s-trans conformation, the stepwise diradical pathway is more energetically

favorable than the concerted one. A stepwise diradical mechanism for the s-cis conformation of 1,3-butadiene is also possible. Both stepwise mechanisms proceed through an initial transition state in which the first bond is formed (8 and 11), leading to the formation of a diradical intermediate (9) and a second transition state (10) that is usually lower in energy than the first one and is more difficult to locate on the potential energy surface. The respective rate determining transition states (8 and 11) for each of the stepwise mechanisms are however, less energetically favorable than the synchronous pericyclic transition state. There is also a possibility of the stepwise diradical pathway diverging to give the trans-cyclohexene product, however the results reported by Johnson[24] indicate that this is a highly improbable process.

From all this, it can be concluded that for the simplest Diels-Alder reaction between ethylene and 1,3-budatiene, the concerted reaction with 1,3-butadiene maintained in the s-cis conformation, passing through a synchronous pericyclic transition state is the most favorable one.

For similar Diels-Alder reactions, the concerted s-cis mechanism is usually preferred, though there are also cases of DA cycloadditions that proceed through the stepwise pathway. For example, stabilization of the diradical TS through delocalization due to conjugation with an adjacent double bond[7, 31-32] or a phenyl substituent on the diene or dienophile[8, 33-34], can lead to an increase in the energetic favorability of the stepwise mechanisms.

It is important to note that the particular reaction shown in Figure 1 is not a very efficient reaction in practice, but it is a good model for illustrating the basic theoretical principles in the DA reaction and the theoretical conclusions are transferable to more complex reaction systems. This simple reaction becomes more efficient with addition of a donor substituent on the diene and an acceptor substituent on the dienophile.

1.2 DEHYDRO DIELS-ALDER REACTIONS

Another way to modify the classic Diels-Alder reaction is by increasing the unsaturation on the diene or the dienophile. Such reactions are known as dehydro Diels-Alder (DDA) reactions[1-8, 34-41]. The most common cases of DDA reactions are illustrated in Figure 2.

Looking at the classic DA reaction, we can imagine that increasing the unsaturation on either the diene or the dienophile, would have an effect on both the mechanism by which the reaction proceeds, and the observed products. The DA cycloadduct in dehydro Diels-Alder reactions is usually a strained cyclic allene. This introduces a second step for the formation of the final product, which is frequently an aromatic six-membered ring. As we can see in Figure 2, hexa-dehydro DA reactions give fully aromatic benzyne derivatives as final products upon isomerization of the initial DA adduct. Isomerization of the DA adduct also leads to the formation of aromatic products, benzene derivatives, in the tetra-dehydro DA reaction. The di-dehydro reaction however, does not necessarily give an aromatic final product. The product of the DA cycloaddition and subsequent isomerization in such reactions is a non-aromatic cyclohexadiene derivative, but the presence of an aromatic benzene derivative formed by the loss of two hydrogens has also been detected in such reaction mixtures, in some cases in significant amounts.[5]

The hexa-DDA and tetra-DDA reactions are very useful in organic synthesis, particularly for preparation of derivatives and polycyclic compounds of benzene (or benzyne). The di-DDA reaction is also a synthetically interesting reaction because it can additionally lead to two different potentially useful products from the same set of reactants. Unfortunately however, the synthetic potential of di-dehydro Diels-Alder reactions is limited by the difficulty in controlling the selectivity for the aromatic or non-aromatic final product, with experiments usually leading to a mixture of both products. One reason for this is that the relationship between the reaction mechanism and the selectivity for the final products, as well as the effect of experimental conditions on the mechanism and the selectivity of the di-dehydro DA reaction, is still not well understood. A more thorough understanding is necessary in order to design systems that will give better selectivity at milder experimental conditions.

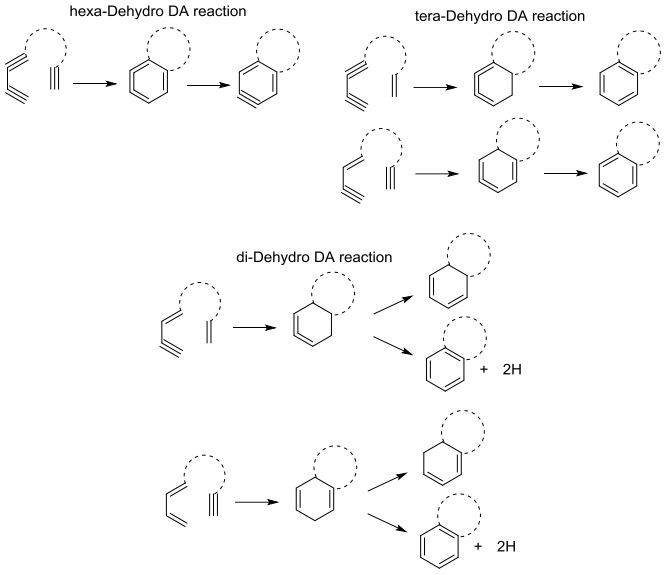

Figure 2 Dehydro Diels-Alder reactions

1.3 INTRAMOLECULAR DIELS-ALDER REACTIONS

The dashed arches in Figure 2 represents a tether connecting the diene and dienophile in the case of intramolecular DDA reactions. The presence of the tether in intramolecular Diels-Alder reactions can affect the mechanism of the DA reaction in two ways: By either enhancing or reducing the rate of the reaction, and by promoting stepwise bond formation.

The effects on the rate of the reaction are a consequence of the favorable or unfavorable entropic effects that result from the conformational properties of the tether or the geometric constraints imposed by the tether. The presence of the tether can for example, make the reaction more favorable through entropic assistance. It can also lead to a reduction in the rate of a reaction if the molecule can form stable conformations in which the diene and dienophile side chains

are positioned in a way that their approach is hindered[41]. If there is electron delocalization present on the tether, or electron withdrawing or donating groups, this can also have an effect on the rate of the reaction.

The presence of the tether between the diene and dienophile in a DA reaction can also introduce a significant amount of asynchronicity in the concerted pericyclic TS, which in some cases can lead to a merging of the stepwise and concerted pathways, with a single TS serving both pathways.[3, 36-37, 42] When in addition to this, there is unsaturation or delocalization through conjugation on the diene or dienophile, the PES of the reaction is significantly different from that of the traditional DA reaction. Such systems can be mechanistically atypical in a variety of ways, resulting in a failure of traditional transition state theory in correctly describing their dynamics. Phenomena such as recrossing[43], multiple competing mechanisms, and mechanisms at the concerted/stepwise boundary have been observed.

1.4 INTRAMOLECULAR DI-DEHYDRO DIELS-ALDER (IMDDA) REACTION OF ENE-YNE SUBSTITUTED HETEROARENES

From all this, it is clear that intramolecular dehydro Diels-Alder reactions have a lot of synthetic potential for the generation of aromatic and nonaromatic polycyclic and heterocyclic compounds. It is also clear that these reactions are more challenging for mechanistic study than typical DA reactions, and the mechanisms by which they proceed are still not fully understood. In particular, there has not been a systematic analysis of the relationship between the physical properties of the substrates, and the rates, yields and selectivity of the IMDDA reaction. This is particularly true for the case of di-dehydro IMDDA reactions. Another common shortcoming of previous studies on IMDDA reactions is that they tend to focus either primarily on the formation of the DA adduct, or on the subsequent isomerization and oxidation steps. If we wish to understand both the rates of these IMDDA reactions and the product selectivity, it is necessary to study both steps in conjunction.

In order to address these questions, I have performed a computational study on a set of de-aromative intramolecular di-dehydro Diels-Alder reactions of 2- and 3- ene-yne substituted heteroarenes. I have also attempted to correlate my computational results with the comprehensive experimental results on these reactions compiled by Ashley Bober and Joseph Winkelbauer in the group of Dr. Kay M. Brummond.

The overall reaction is illustrated in Figure 3. As can be seen in Figure 3, the IMDDA reaction of 2- and 3- substituted alkenyl heteroarenes consists of the two main steps discussed in the introduction for DDA reactions: In the first step, the intramolecular Diels-Alder cyclization gives the dearomatized Diels-Alder adduct. Dearomatization in this case refers to the additional loss of aromaticity in the heteroarene when forming the non-aromatic Diels-Alder adduct. In the second step, either an intramolecular hydrogen atom abstraction and isomerization takes place to give the isomerized product, in which the aromaticity of the heteorarene has been restored. Or, a concerted loss of H_2, gives the fully aromatic oxidized product. Isomerization of the DA adduct, can also lead to the formation of another product that we refer to as the diene product. The diene product has only been observed in DMF. It is an unreactive

intermediate. It does not go to product or reactant. This was confirmed experimentally by isolation of the DA adduct in DMF that gave a mixture of oxidized product, isomerized product, and the diene product.

It is reasonable to assume that the initial step to form the Diels-Alder adduct (step 1) is the most energetically demanding, and is thus the rate-determining step for the IMDDA reaction. On the other hand, the final product selectivity is most likely a consequence of the elementary processes in the second step (step 2) of the reaction.

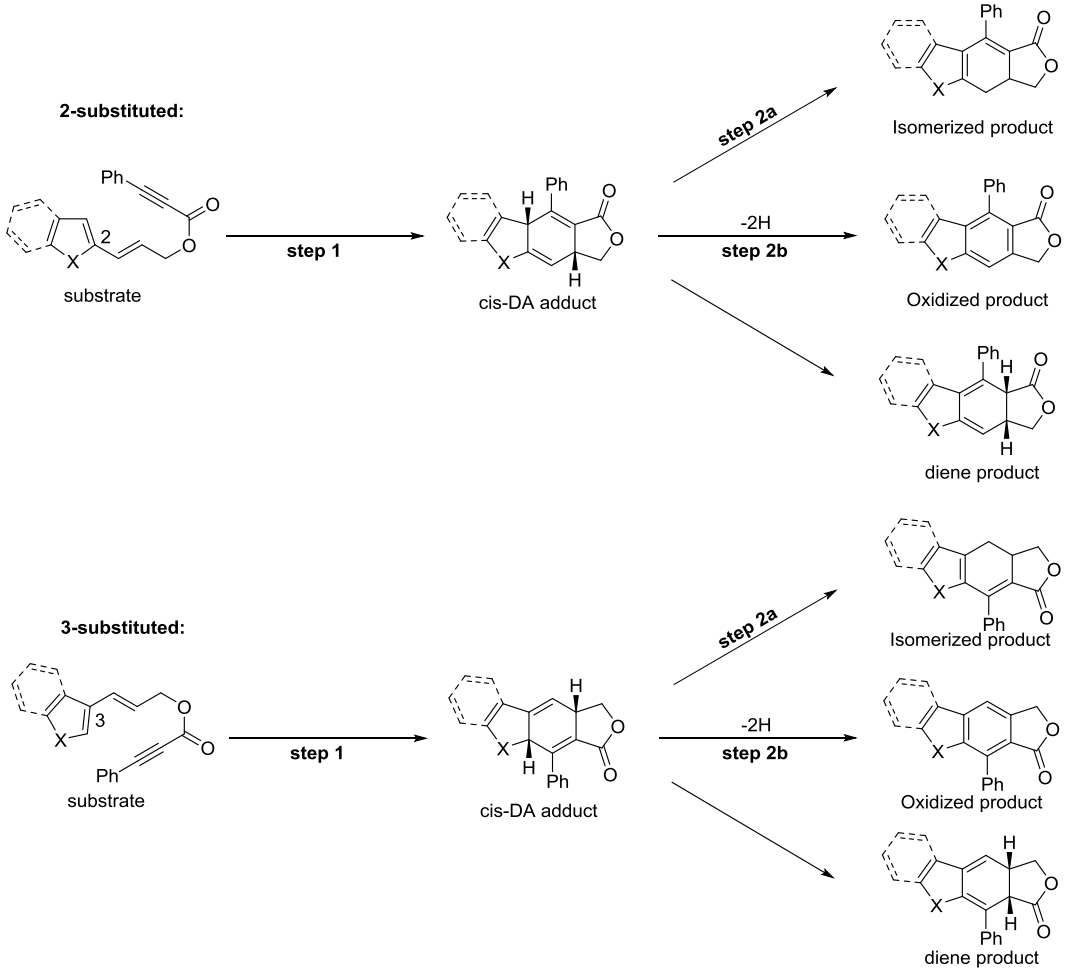

Figure 3 The IMDDA reaction of C2 and C3 ene-yne substituted heteroarenes

In this thesis, I have focused on the set of substrates shown in Figure 4. In the naming of the studied compounds I have adopted the following terminology: Each of the compounds is named according to the general scheme n-name-e/k(t), where n represents the position of substitution of the tether, followed by a short form of the name of the heteroarene. This is followed by the letter e or k, e indicating an ester tether, and k indicating a ketone tether. Finally, t indicates that the hydrogen atom on the nitrogen in pyrrole and indole has been replaced by the tosyl group. For the names of the heteroarene, thioph stands for thiophene, BT stands for benzothiophene, pyr stands for pyrrole, and ind stands for indole. In addition to this, in the naming convention of the SI, -add stands for DA adduct, -ox stands for

oxidized product, and -isom stands for isomerized product. CS_TS means closed shell TS, OS_TS means open shell transition state, and s-cis and s-trans, refer to the conformation on the diene.

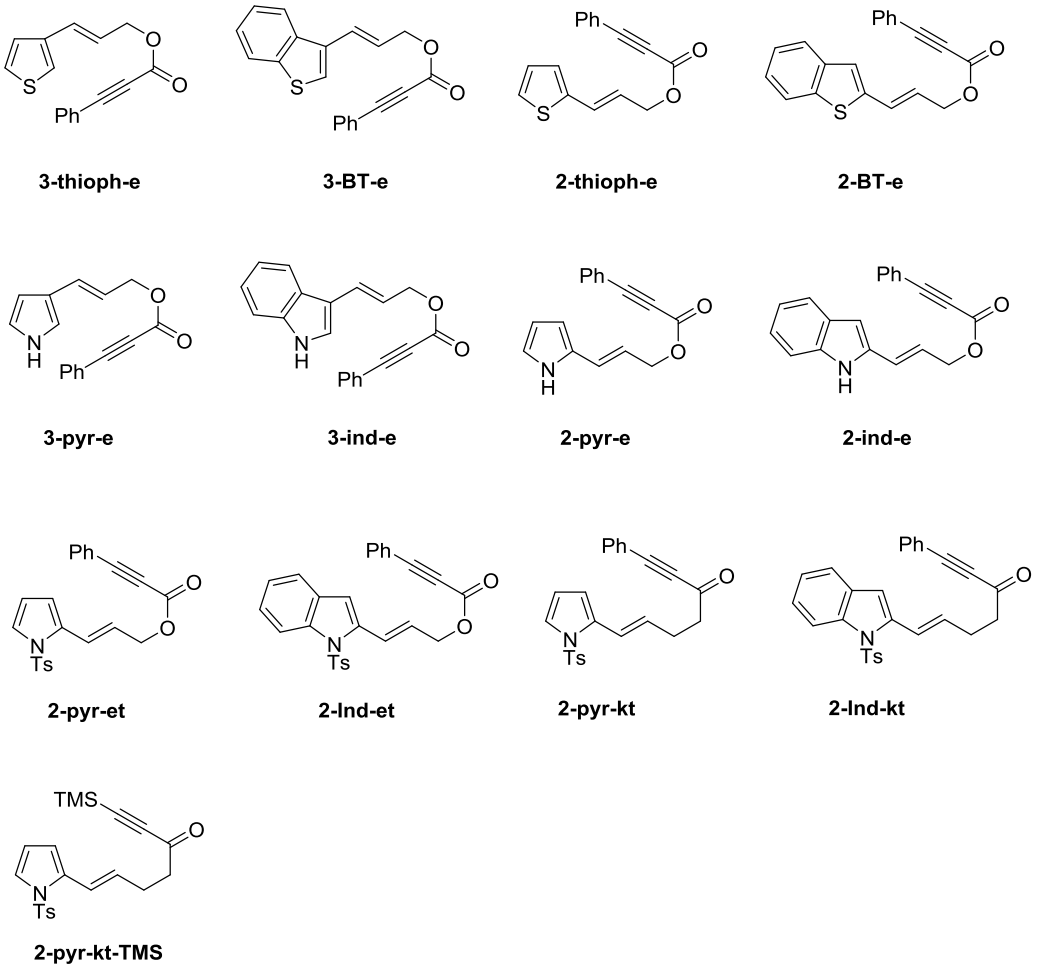

Figure 4 The list of substrates in the study of the IMDDA reaction of 2- and 3- ene-yne substituted heteroarenes

The substrates were selected either because experimental results were available (3-thioph-e, 3-BT-e, 2-thioph-e, 2-BT-e, 2-pyr-et, 2-ind-et, 2-pyr-kt, 2-ind-kt), or for completeness in the theoretical comparisons (3-pyr-e, 3-ind-e, 2-pyr-e, 2-ind-e). The substrates for which experimental evidence is available, were chosen by the experimental researchers for several reasons. An ester tether was chosen because based on previous reactions with heteroarenes, the ester tether ones showed a larger range of variability depending on tether attachment position. They had conducted the experiments with Sulphur- and nitrogen- containing heteroarenes only, because previous experiments had shown that oxygen-containing heteroarenes gave poor yields in both the preparation of the substrate, and the cycloaddition step.[1] In order to study the effects of aromaticity, both thiophene and benzothiophene, and pyrrole and indole precursors were chosen. In addition to the interest in increasing the mechanistic diversity for the set of IMDDA reactions, including the benzofused heteroarenes, afforded a wider range of practically useful compounds.

For the nitrogen heteroarenes, the tosyl group had been used as a protective group in the initial synthesis of the substrates, and it was interesting to see the effect of the presence of the tosyl group on the heteroatom. However, for the 3-substituted species low yields and high reaction temperatures in the preparation of the aromatic product were observed. This was attributed unfavorable steric effects in the DA transition state between the tosy group and the aryl group on the alkyne. Because of this only the 2-substituted pyrrole and indole were included in the experimental study.

This selection of substrates reflects the goals stated in the introduction. I am interested in studying the effect of the additional aromaticity due to the presence of the benzene ring fused to the heteroarene, the effect of tether attachment position, and the effect of the identity of the heteroatom on the IMDDA reaction. In particular, I am interested in the relationship between these factors and the mechanism of the DA cycloaddition, and with that, the rate of the reaction. I am also interested in developing a greater understanding of the way in which these factors are related to the selectivity for the final oxidized and isomerized product.

It is interesting to note that the experimental results indicate that only the cis-adduct has been observed in the reaction mixture. This leads me to wonder why this might be the case. Is the trans-adduct not formed, or is it just not experimentally observable? And, is this a sign that a stepwise mechanism does not occur for any of the reactions, or is it possible that a stepwise mechanism does occur in some cases, but a trans-adduct is not formed? This experimental result is not necessarily expected because the substrates in the studied IMDDA reactions have all the characteristics of diene-dienophile pairs that would be characterized by a reaction PES significantly different from that of the traditional DA reaction. Both the diene and dienophile are conjugated with aromatic substituents, a connecting tether facilitates an intramolecular reaction, and the dienophile is acetylene, which is more unsaturated than ethylene. Although a concerted s-trans TS for the DA cycloaddition is not possible, both the s-cis and s-trans stepwise transition states are not unfavorable, and the trans-adduct although more energetically unfavorable than the cis-adduct, is not so strained, that the reaction is endothermic. Because of this, we cannot exclude all possibility of a stepwise mechanism, or the formation of a trans-adduct based on theoretical principles. As we will later see, DFT calculations confirm this.

2.0 COMPUTATIONAL METHODS

In order to answer these questions I performed a series of DFT (density functional theory) calculations using the Gaussian 16[44] software package. I chose the methods for the calculations in step 1 and step 2 based on the specific requirements for the properties studied. For the transition state calculations, it is important to consider that the transition state contains partially formed bonds that require both non-dynamical and dynamical electron correlation for a proper treatment[45]. A method that does not account for electron correlation properly will not give a reliable description of the transition state geometry. Furthermore, a correct treatment of electron correlation is more essential for the transition state than for the ground state geometry. A method that does not account for electron correlation equally well in the ground state and in the transition state, will not give reliable free energies of activation. It is very expensive to achieve this computationally with *ab initio* methods, where calculations using high level methods such as CASPT2, CI, MP4, and CC are required. On the other hand, DFT calculations with hybrid GGA functionals can offer a good treatment of electron correlation in the transition state and ground state at a much lower computational cost. The B3LYP[46-49] functional, combining Becke's 3 parameter exchange correlation hybrid with GGA LYP dynamical correlation has repeatedly been shown to perform well for the study of transition states in DA reactions[50-51]. M062X[52], a meta-GGA hybrid functional is also frequently used in mechanistic studies on DA reactions.

I started out by optimizing the geometries of the transition states for the s-cis concerted, s-cis stepwise, and the s-trans stepwise DA cycloaddition mechanisms and calculating the free energies of activation at the (U)M062X/6-311+g(d,p)//(U)M062X/6-31+g(d) and at the (U)B3LYP/6-311+g(d,p)//(U)b3lyp/6-31+g(d) levels of theory[53-54]. For the open-shell species, I performed the calculations using the unrestricted formalism and breaking of the α-β and spatial symmetries. A test for the stability of the wave-function confirmed that the closed-shell singlet is the lowest energy wave-function for the closed-shell species, and an open-shell singlet is the lowest energy wave-function for the open-shell species.

The correlation with experiment was, much less satisfactory with the M062X functional, and it seemed like M062X consistently overestimated the free energies of activation for the stepwise transition states, and underestimated the degree of asynchronicity for the concerted transition states, resulting in concerted free energies of activation that show no correlation with experiment (see Figure B1 in Appendix B). This is not surprising. M062X is not the best performer for open-shell systems among the M06 family of functionals[55-56], possibly due to the very high contribution from HF exchange, and it is known to overestimate the free energy of activation for open shell-singlet TSs[57-58]. On the other hand, the B3LYP functional is known to give very good correlation with experiment for transition state geometries

and free energies of activation for Diels-Alder reactions[45], so I decided to proceed with the transition state calculations using the B3LYP functional.

Because it initially seemed like the trans-adduct was formed in DMF, a very polar solvent, but not in other solvents, we assumed that the polarity of the solvent might have an effect on the mechanism by which the reaction proceeds. I hypothesized that a stepwise mechanism might be preferred in polar solvents, and a concerted mechanism in nonpolar solvents. Because of this I performed the initial TS calculations (the calculations for 2-thioph-e, 2-BT-e, 3-thioph-e, 3-BT-e, 2-ind-et, and 2-pyr-et) in the two solvents in which the majority of experiments were carried out: DMF (a highly polar solvent) and o-DCB (which has a much lower dielectric constant than DMF). I also performed calculations in the gas phase, for comparison with the solvent calculations. Even though we know now that the trans-adduct has actually not been observed experimentally, the results of these calculations are still useful for an initial analysis on the effect of solvent on the free energies of activation. However, because the initial calculations indicated that the solvent does not have an effect on whether the s-cis or s-trans TS is more energetically favorable, or on the relative favorability of the DA cycloaddition step for the different substrates, I proceeded to calculate the remaining transition states in gas phase only (2-ind-e, 2-pyr-e, 3-ind-e, 3-pyr-e), or in gas phase and o-DCB solvent where comparison with the experimental rates determined in o-DCB was needed (2-ind-kt, 2-pyr-kt, 2-pyr-kt-TMS).

For step 2, the studies on the effect of experimental conditions on product selectivity indicate that the selectivity is under kinetic rather than thermodynamic control, and depends on the mechanisms by which the isomerized and oxidized products are formed. In addition to this, the results of these studies led the experimental researchers to hypothesize that the isomerized product most likely forms through an anionic mechanism. This was supported by the fact that solvent polarity was found to influence the product selectivity. For example in the reaction of 3-BT, DMF, a polar solvent, was found to promote the formation of the isomerized product, whereas in the much less polar o-DCB, the oxidized product was formed in a higher yield. Furthermore, the presence of water in DMF resulted in an increased yield for the isomerized product, compared to reactions in DMF only, and experiments with D_2O resulted in significant deuterium incorporation. A kinetic isotope effect study on the reaction of 3-BT in o-DCB, resulted in decreased yields for both the isomerized and oxidized product, indicating the importance of hydrogen mobility. These results suggest that water could be playing a role in the hydrogen abstraction for the formation of the isomerized product in polar, protic solvents, and it provides additional support for the hypothesis that the isomerized product could form according to an ionic mechanism. In addition to the effect of the addition of water in the solvent, increasing the initial concentration of the DA adduct also increased the amount of isomerized product formed. The concentration effect seems to indicate that the mechanism for the formation of isomerized product can also be propagated through interactions with intermediates present in the reaction mixture. In addition to this, experiments on the effect of atmosphere, revealed that oxygen has an accelerating effect on the rate at which the oxidized product is formed, indicating that the oxidized product might form through a radical mechanism. Although it appears that experimental evidence supports an ionic mechanism for the formation of the isomerized product, and a radical mechanism for the formation of the oxidized product, a radical mechanism for the formation of the isomerized product can also be considered, as well as the possibility of an ionic mechanism or unimolecular hydrogen abstraction for the formation

of the oxidized product. The plausible mechanisms proposed by the experimental researchers for the formation of the isomerized and oxidized product based on these results are summarized in Figure A1 in Appendix A.

In order to test these hypotheses, I calculated the gas phase acidities and BDEs (bond dissociation energies), to see whether the trend would support an anionic or radical mechanism for the formation of the isomerized or oxidized product. The chemical equations according to which the BDE and acidity were calculated as well as the dissociating protons for the 2- and 3- substituted DA adducts are represented in Figure 5. I also analyzed the relative free energies of the da adduct and the oxidized, isomerized, and diene product, with respect to the substrate, in order to get an initial idea of the effect of solvent and the identity of the diene heteroarene on their relative stability, and to confirm that the selectivity is influenced by the relative free energies of reaction.

B3LYP however, does not perform well for reaction energies. M062X has been shown to give a much better prediction of reaction energies. Houk has suggested that the error when using B3LYP and other functionals that underperform in this way is a result of its inability to properly treat σ-π transformations, and this leads to particularly large errors in the free energies of reaction for reactions where the number of σ and π bonds is not conserved[59]. Because of this, for the ground state relative free energies, and for the gas phase acidities and BDEs, I performed the calculations at the M062X/6-311+g(d,p)//M062X/6-31+g(d) level of theory.

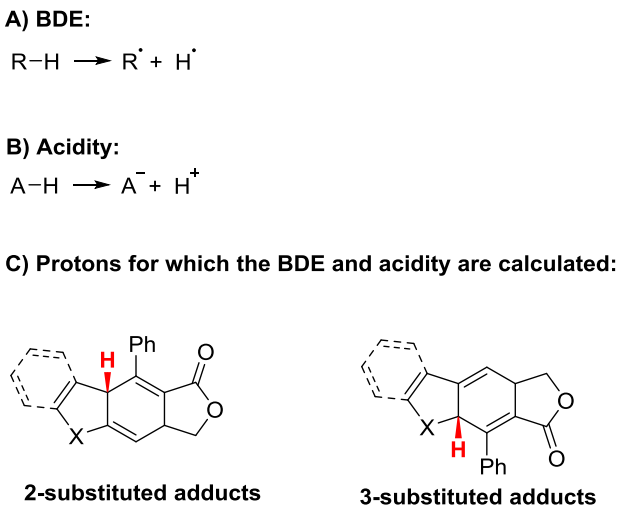

Figure 5 A) Chemical equations according to which the BDE is determined B) Chemical equation according to which the acidity is determined C) Protons for which the BDE and acidity have been computed

I performed all the calculations in solvent using the SMD solvation model[60]. SMD is an implicit solvation model, so it cannot offer a detailed understanding of the role that solvent plays if it has a more active role in the reaction studied. It can however, provide an initial idea of the effect of solvent polarity on the relative energies of activation and stabilities of the products in these reactions. This is adequate for the set of IMDDA reactions studied in this thesis, because experiments on the effect of solvent indicated that solvent polarity was the main solvent property that had an effect on the observed reactivity.

I obtained the geometries, relative free energies, and free energies of activation at the standard temperature in Gaussian, 298.15 K. I also determined the free energies, enthalpies, and entropies of activation, for the substrates for which experimental rate data was available, at 363 K, the average temperature at which the experiments for the rates of reaction were carried out, using the goodvibes program[61-65], with the harmonic approximation. The quasiharmonic approximation did not seem to improve the results. I used the CYLview[66] and Molden[67] programs for visualization of the optimized geometries.

Finally, I calculated the nuclear independent chemical shift (NICS)[68-69] of the substrates, DA transition states, DA adduct, isomerized, and oxidized product, in order to quantify the degree of breaking and restoring of the aromaticity at these points along the reaction coordinate, and to test whether the aromaticity is related to the free energies of activation, or the selectivity in the reaction. For these species, I determined the NICS(1)zz index, which has been shown to be a reliable measure of the aromatic stabilization energies in planar π-systems[68-70]. NICS(1)zz values correspond to the component of the NICS tensor that is perpendicular to the plane of the ring, calculated at a 1 angstrom distance from the center of the ring, where the local shielding effects are negligible, and the observed chemical shift is primarily a consequence of the π-current[71]. This value can be read from the Gaussian output when the input geometry for the NMR calculation is such that the atoms of the ring are positioned in the xy plane, and the center of the ring is at the center of the Cartesian coordinate system. To maintain agreement with the conventions for the chemical shift, the negative of this value is reported. In order to prepare the input geometries, I wrote a short C++ program that moves the unweighted center of the ring to the center of the coordinate system, finds the best fit for the plane of the atoms of the ring, places the ghost atoms at one angstrom perpendicular to the plane of the ring, and reorients the molecule so that the ring lies in the xy plane. I have uploaded the program to my GitHub page[a]. I performed the NICS calculations at the B3LYP/6-311+g(d,p)//B3LYP/6-31+g(d) level of theory, using the NMR keyword in Gaussian.

[a] https://github.com/ElenaKusevska/NICS_prepare_input/tree/master/using_regression_plane

3.0 RESULTS AND DISCUSSION

3.1 COMPUTATIONAL RESULTS FOR THE DA CYCLOADDITION STEP

3.1.1 Geometries of the identified DA transition states

For the first step in the IMDDA reaction, the formation of the DA adduct, I attempted to identify the s-cis closed shell transition state and the s-cis and s-trans conformations for the diradical transition state for the substrates considered in this study. I did not consider the s-trans closed shell transition state because it is not very probable, and it would not lead to the desired product. I considered the s-cis closed shell transition states as representative of a concerted DA pericyclic transition state, and the open shell transition states as representative of a stepwise DA transition state. Inspection of the vibrational frequencies confirmed that the s-cis closed shell is a concerted transition state, corresponding to the formation of both bonds, and the open shell transition states are stepwise, corresponding to the formation of the first bond only.

I successfully identified the concerted s-cis TS for all of the substrates. For the majority of the substrates I have also identified the s-trans stepwise TS. The s-cis stepwise transition states were very difficult to locate on the potential energy surface because the geometry optimizations frequently collapse to the closed shell singlet due to their geometric similarity with the corresponding s-cis concerted TSs. Because of this difficulty, I have only been able to optimize the geometry of the s-cis open-shell transition states for 2-thiophene-e, 2-pyr-e, and 2-pyr-et in gas phase, for 2-BT-e, and 2-ind-e in o-DCB, and for 2-thioph-e and 2-ind-e in DMF, at the (U)B3LYP/6-31+g(d) level of theory. The free energies of activation of all the identified transition states, determined at the default temperature in Gaussian, 298.15 K are summarized in Table B1, in Appendix B.

The geometries of the transition states for some representative substrates, optimized at the (U)B3LYP/6-31+g(d) level of theory in gas phase are shown in Figure 6 and Figure 7, and the geometries of the BT-e TSs optimized in o-DCB are shown in Figure 8. The results for the other transition states are analogous. There was no considerable deviation in the optimized geometries with the inclusion of solvent effects modeled with the SMD solvation model.

Looking at Figure 6, Figure 7, and Figure 8, first of all, we can see that all of the closed shell transition states are highly asynchronous. They are nonetheless, still concerted. We can also see that all three transition states have almost the same length for the shorter bond that is more fully formed, but the second bond is longer in the diradical TSs. In particular, we can see that in every case the second bond is longer in the s-cis diradical TSs, compared to the s-cis closed-shell TSs, indicating that in spite of their geometric similarity these are indeed two different transition states,

with a different degree of concertedness. It is also interesting to note that among the s-cis concerted TSs, the second bond is shorter for the 3-substituted species, compared to the 2-substituted species, i.e. the s-cis concerted TSs are slightly more synchronous for the 3-substituted species. It appears as though the particular conformational properties of the tether and hetereocycle diene are such that for the 3-substituted species, concerted bond formation from an s-is TS geometry is promoted.

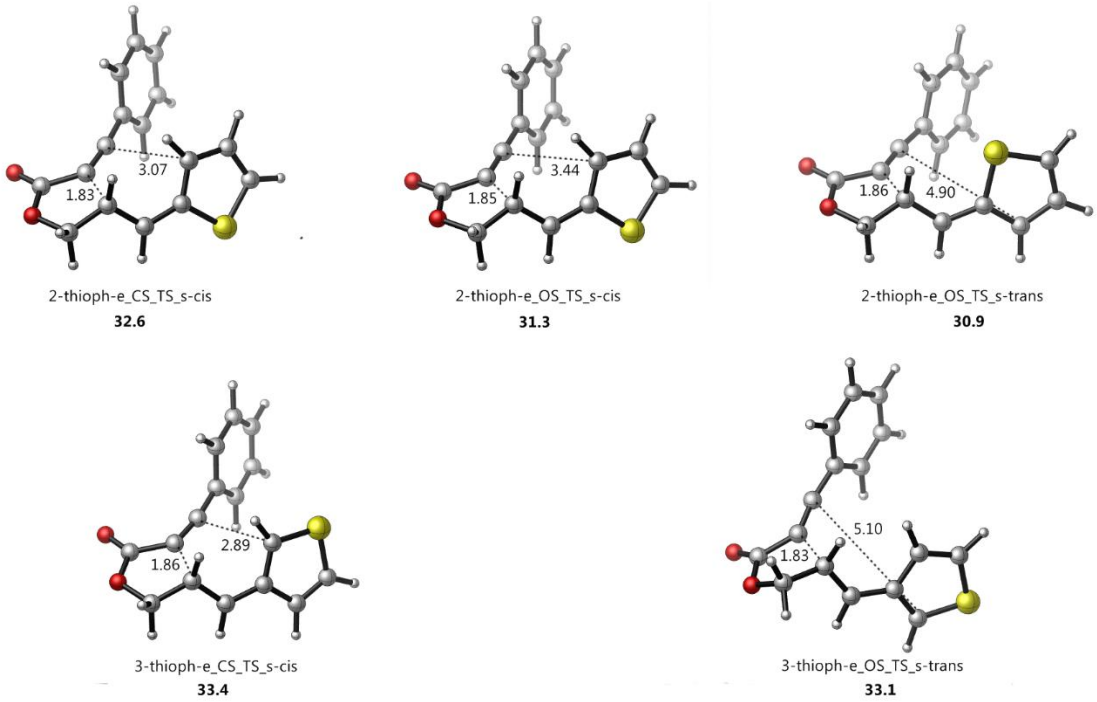

Figure 6 2-thioph-e and 3-thioph-e TSs for the formation of the DA adduct optimized at the (U)B3LYP/6-31+g(d) level of theory in gas phase at 298.15 K. The reported bond distances are in Angstroms and the free energies of activation are in kcal/mol

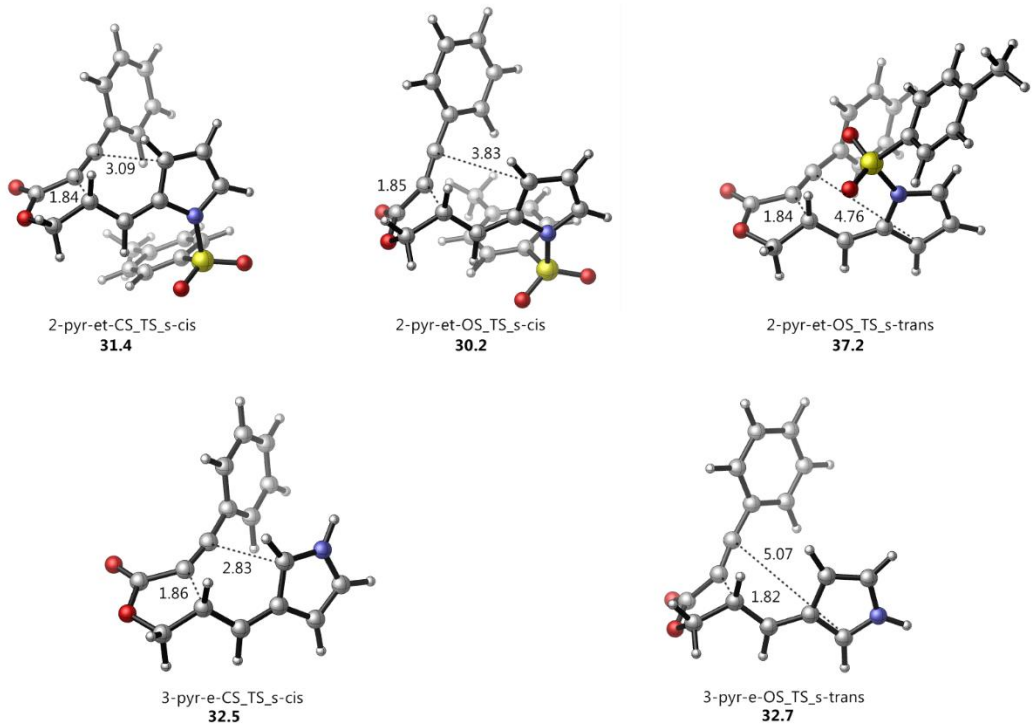

Figure 7 2-pyr-et and 3-pyr-e TSs for the formation of the DA adduct optimized at the (U)B3LYP/6-31+g(d) level of theory in gas phase at 298.15 K. The reported bond distances are in Angstroms and the free energies of activation are in kcal/mol

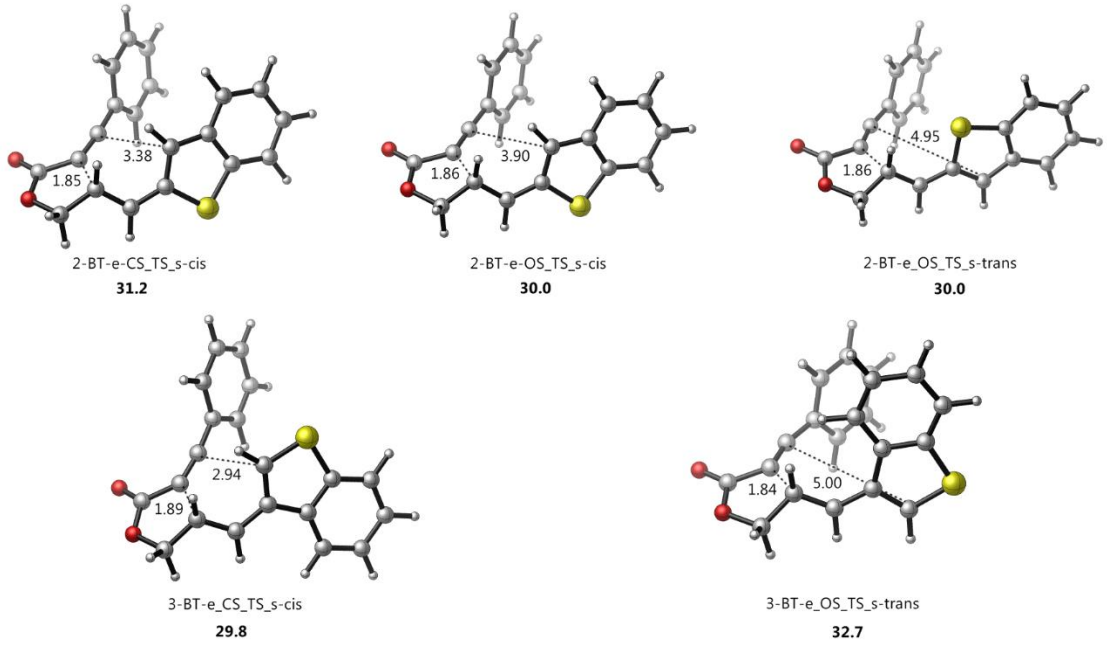

Figure 8 2-BT-e and 3-BT-e TSs for the formation of the DA adduct optimized at the (U)B3LYP/6-31+g(d) level of theory in o-DCB at 298.15 K. The reported bond distances are in Angstroms and the free energies of activation are in kcal/mol

3.1.2 Free energies of activation of the identified transition states

I began by optimizing the s-cis and s-trans TSs of 3-BT-e, 2-BT-e, 3-thioph-e, 2-thioph-2, 2-ind-et, and 2-pyr-et in gas phase, DMF, and o-DCB solvent because of our initial hypothesis that the solvent might have an effect on whether the concerted or the stepwise transition state is more energetically favorable. However, there is no evidence to suggest that the inclusion of solvent using the SMD solvation model, at this level of theory, has any effect on which of the transition states is the most favorable for a given substrate. For example, we can see in table B1 that in all the cases where the s-cis stepwise TS has been identified, it is slightly lower in energy than the s-cis concerted TS, regardless of whether solvent is present or not. Furthermore, looking at the results for the s-cis concerted and the s-trans stepwise TSs for the different solvents summarized in Figure 9, we can see that solvent also does not play a role in whether the s-cis or the s-trans conformation is more stable. This result is more clearly evident in Figure 10, and in Figure 11 we can see that although there is an interesting solvent effect, the inclusion of implicit solvent affects the free energy of activation of the s-cis and the s-trans TSs in the same way. The free energy of activation is increased in DMF compared to the gas phase, and in o-DCB the reaction is more favorable than in gas phase.

Looking at the data in Figure 9, we can see that there are some trends in the free energies of activation with respect to the effect of the position of substitution and the presence of a benzene ring fused to the heteroarene diene. These effects are evident in Figure 10, but they are better illustrated in Figure 12, where the difference in the free energy of activation between the s-cis concerted and s-cis stepwise transition states for the sulfur and nitrogen heteroarenes with an ester tether and no tosyl group on the nitrogen at the the (U)B3LYP/6-311+g(d,p)//(U)b3lyp/6-31+g(d) level of theory in gas phase at 298.15 K is shown. We can see that for 2-BT-e, 2-thioph-e, and 2-ind-e the s-trans transition state is preferred, and this is more pronounced for the benzofused heterocyclic dienes. On the other hand, for 3-BT-e and 3-ind-e, the s-cis TS is more favorable, and there is no significant effect for 3-pyr-e and 3-thioph-e. This is better summarized in Figure 13, where we can see that going from the 2-substituted to the 3-substituted species has a reverse effect on the s-cis closed shell and the s-trans open shell TSs, and this is particularly evident for the benzofused heteroarenes. For example, the s-cis concerted transition state of 3-BT-e is more favorable than the s-cis concerted TS for 2-BT-e, and the s-trans stepwise TS of 3-BT-e is more unfavorable than the s-trans TS of 2-BT-e. Similarly, the s-trans TS of 2-thiophene is more favorable than that of 3-thiophene. However, the s-cis TS is also destabilized in going from 2-thioph-e to 3-thioph-e, but to a lesser extent.

Looking at the results in Figure 12 and Figure 13, we can see that the presence of the bezene ring fused to the heteroarene also has an effect on the observed trend. The s-cis closed-shell TS is particularly stabilized in the case of the 3-substituted benzofused species, 3-BT-e and 3-ind-e, but this is not the case for 3-thioph-e and 3-pyr-e.

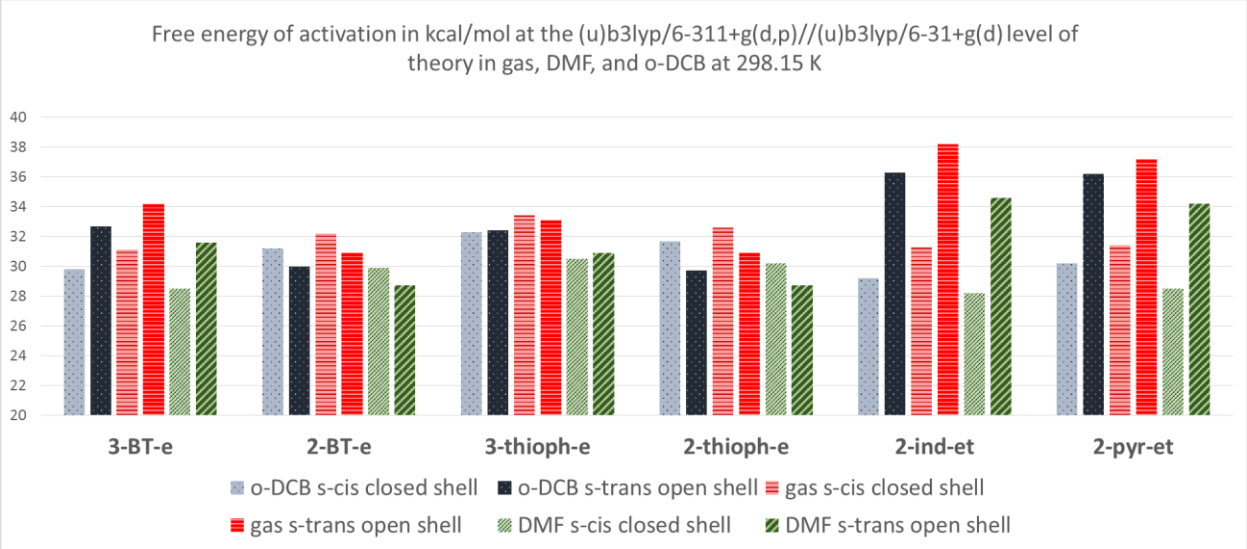

Figure 9 Summary of the free energies of activation in o-DCB, gas, and DMF

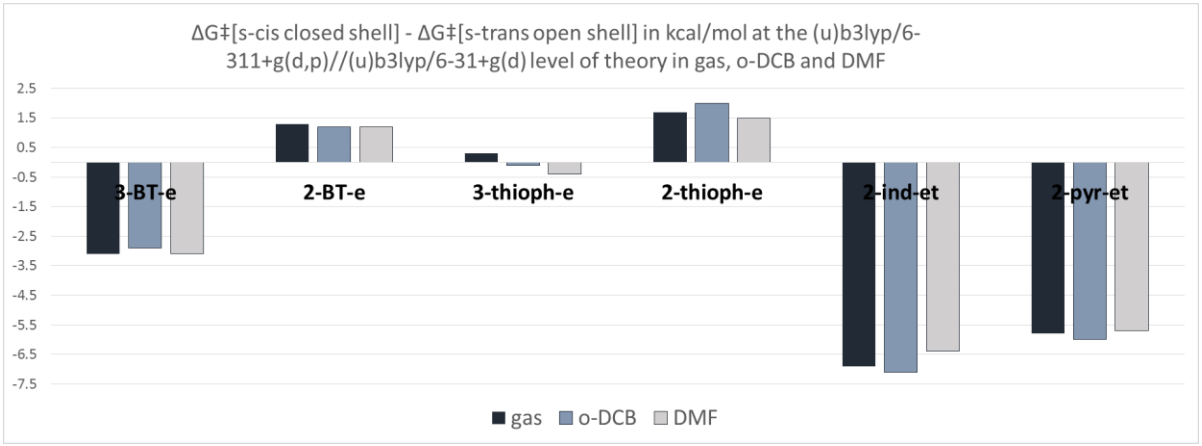

Figure 10 Effect of solvent on the relative stability of the s-cis CS and s-trans OS TSs

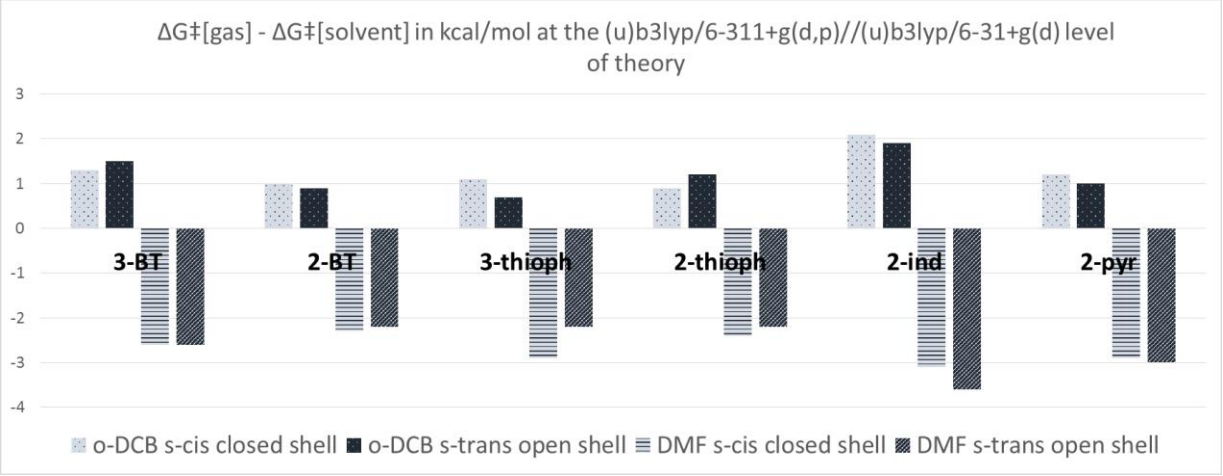

Figure 11 Effect of solvent on the free energies of activation of the s-cis CS and strans OS TSs

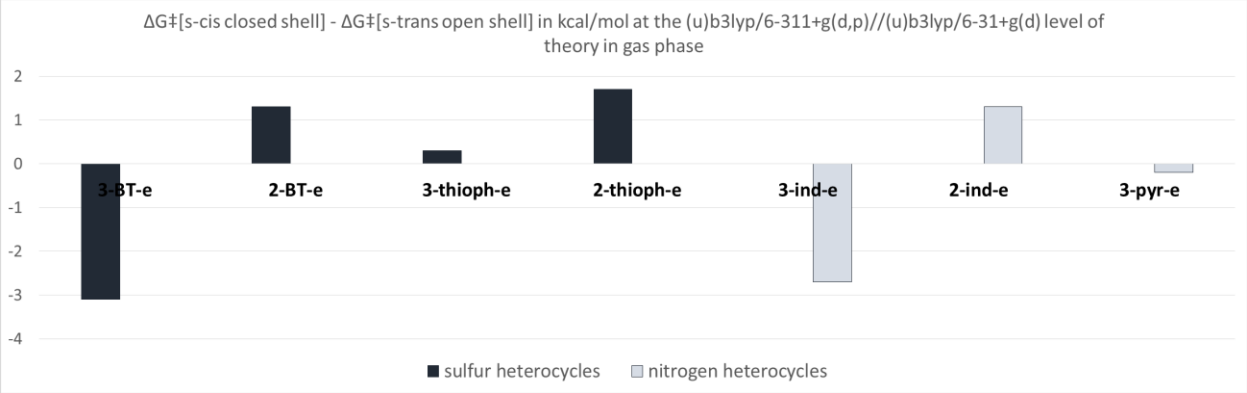

Figure 12 Diference between the free energy of activation of the s-cis CS and the s-trans OS TS

The overall trend when there are no additional steric effects like those from the tosyl protecting group on the nitrogen, can be summarized in the following way: For the 3-substituted benzofused species, the s-cis TS is stabilized and the s-trans conformation is destabilized, and for the 2-substituted species, the s-trans TS is stabilized and the s-cis TS is destabilized. This is most likely primarily a consequence of the particular conformational properties of the tethers that promote the s-cis concerted pathway in the 3-substituted species, particularly for 3-substituted benzofused species, and a stepwise pathway for the 2-substituted species. Considering that the 3-BT s-cis CS TS is more synchronous than the 2-BT CS TS to a greater degree than is the case for the 2-substituted substrates, it is possible that the DA cycloaddition is characterized by a greater degree of concertedness for the 3-substituted compared to the 2-substituted heterocyclic dienes. These two effects, the effect of the presence of the additional benzene ring in the benzofused species, and the tether attachment position, seem to be the main contributors to 3-BT having the most favorable s-cis concerted transition state and 2-thiophene having the most favorable s-trans stepwise TS among the sulfur-heteroarenes.

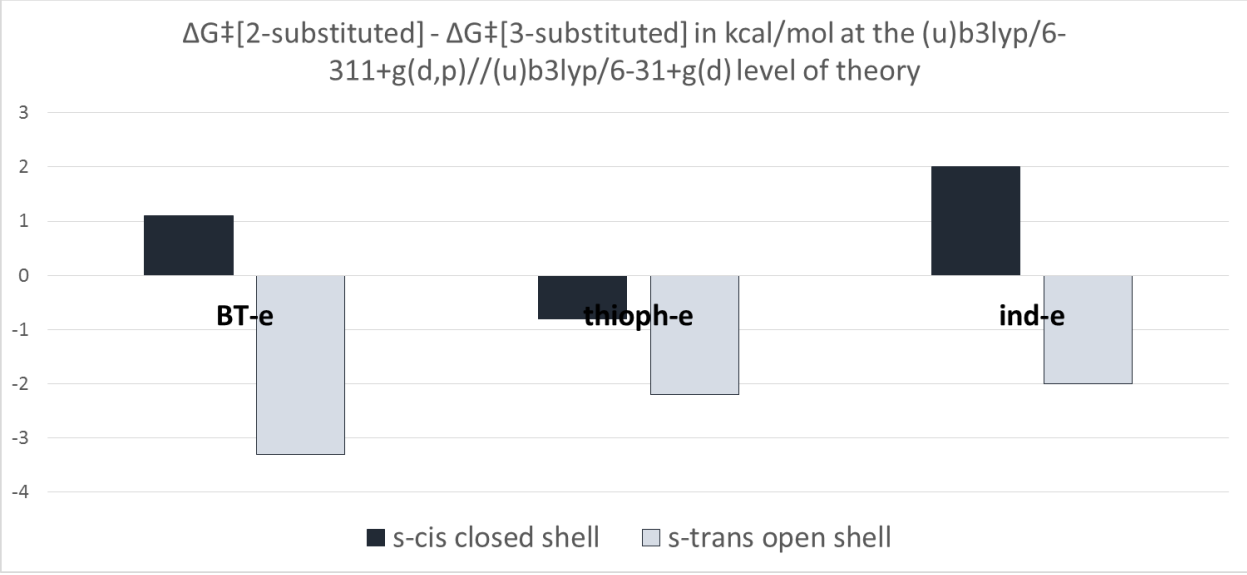

Figure 13 Differemnce between the analogous 2-substituted and 3-substituted transition states

3.1.3 Aromaticity of the diene heteroarene

Because the effect of the tether attachment position on the free energies of activation is enhanced by the presence of a benzene ring fused to the heteroarene, and because the presence of the benzene ring has an effect on the relative stability of the s-cis and the s-trans transition states, I considered the possibility that the observed effects are related to aromaticity. I considered the possibility that the position of substitution and the conformation of the diene might have an effect on the aromatic stabilization energy that could have an effect on the relative favorability of the transition states.

This is however, not the case. The NICS(1)zz of several representative species are presented in Table 1. Because the transition state is not a planar molecule the chemical shift on the outer side of the ring might be different from that on the inner side of the ring, so it is necessary to make a distinction between the different sides of the ring. The directions in space corresponding to NICS(1)zz-up and NICS(1)zz-down are illustrated in Figure 16. The directions for the other species are determined in an analogous way. As we can see in Table 1, the differences in both the free energies of activation and the differences in the NICS(1)zz values for these species are very small. Nonetheless, if we plot these values (Figure 15), it appears like there is a trend where the relative free energy (or free energy of activation) is higher for the species with higher aromatic stabilization energies. This seemingly counterintuitive result simply indicates that aromaticity has no effect on the free energy of activation for the different transition states. Whether the s-cis or s-trans TS is more favorable for a given heteroarene diene and position of substitution is not related to the aromaticity of the heteroarene.

The trend observed in Figure 15 is simply a consequence of the fact that the studied reactions are dearomative cycloadditions, and the product of the cycloaddition, the DA adduct, is not aromatic. Because of this, the further along the reaction coordinate a species is, the closer it is to the final product, and so the relative free energy and the aromaticity both decrease. A representative example of the changes in the aromaticity of the diene heteroarene throughout the course of the IMDDA reaction is given in Figure 16. As we can see, the transition state is very early, and the aromaticity of the diene heteroarene is not significantly different from that in the starting heteroarene. The fact that the aromaticity in the transition state is not significantly distorted from the starting and that the aromatic stabilization energies do not vary significantly among the different transition states for a given substrates is the reason why the free energies of activation do not depend on the aromaticity of the diene heteroarene in the TS.

Table 1 Computed NICS(1)zz values of the transition states and intermediates in the IMDDA reactions of thiophene and benzothiophene, computed in gas phase fo the thiophene species and in o-DCB for the benzothiophene species

	Species	Grel	NICS(1)zz-out	NICS(1)zz-in
2-thioph	2-thioph-e-CS_TS_s-cis	32.6294	-23.2383	-22.6085
	2-thioph-e-OS_TS_s-cis	31.2745	-22.7084	-22.3037
	2-thioph_e-OS_TS_s-trans	30.8705	-22.0871	-21.6480
	2-thioph-e_ OS-intermediate_s-cis	26.9	-17.4679	-17.1553
	2-thiops-e_OS-intermediate_s-trans	26.738	-16.7702	-16.5307
3-thioph	3-thioph-e_CS_TS_s-cis	33.3669	-23.6706	-23.0674
	3-thioph-e_OS_TS_s-trans	33.1007	-21.5752	-21.8692
2-BT	2-BT-e-CS_TS_s-cis	31.2018	-17.7056	-16.9835
	2-BT-e-OS_TS_s-cis	30.4495	-16.9521	-16.6285
	2-BT_e-OS_TS_s-trans	29.994	-16.4123	-15.8564
	2-BT-e_ OS-intermediate_s-cis	25.7484	-12.9341	-12.3990
	2-BT-e_OS-intermediate_s-trans	25.4711	-12.2503	-11.8006

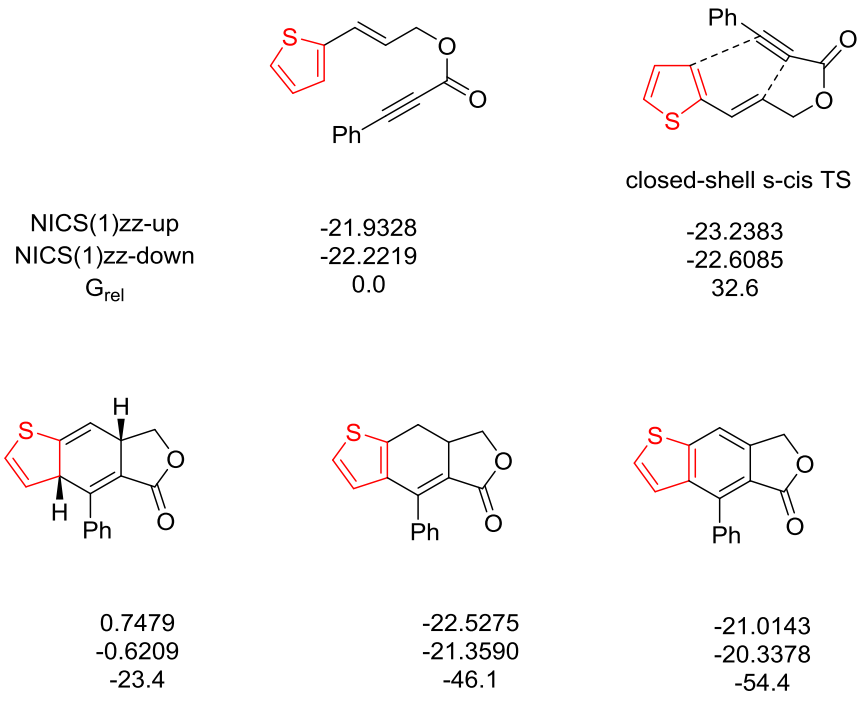

Figure 14 Computed NICS(1)zz values of the heteroarene in the substrate, CS TS, DA adduct, isomerized, and oxidized form of 2-thioph-e

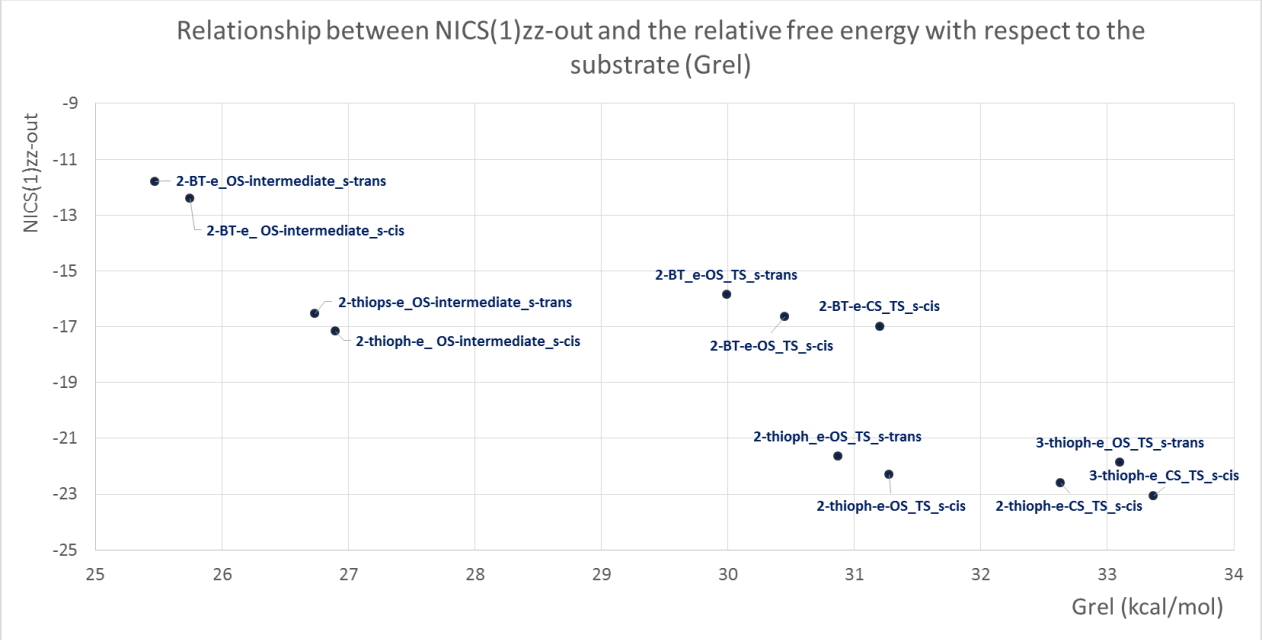

Figure 15 Correlation between the NICS(1)zz values and the relative free energy (free energy of activation)

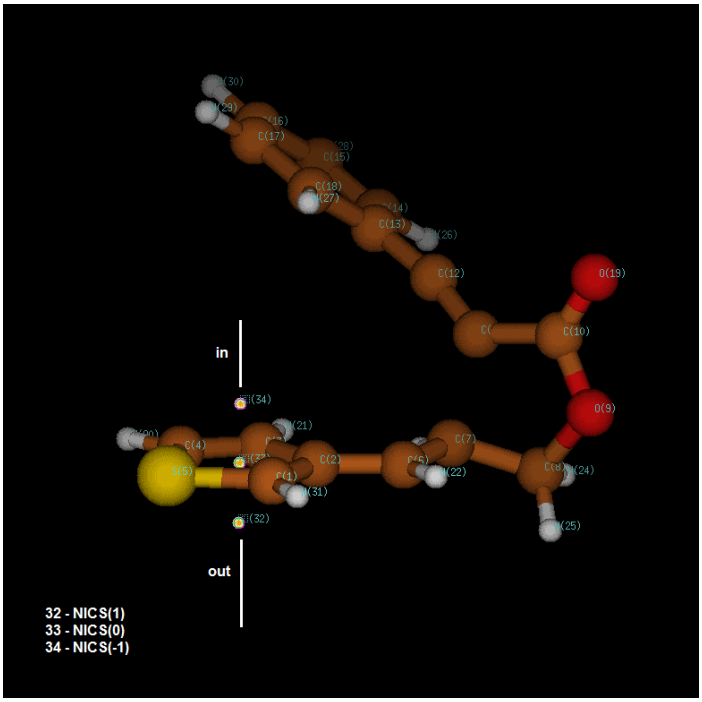

Figure 16 Definition of the "in" and "out" direction along the z-axis in the TS

3.1.4 Proposed mechanism for the DA cycloaddition

For 2-thioph-e and 2-BT-e I have identified the s-cis stepwise transition states as well as the intermediates for the stepwise mechanism. The proposed mechanisms for the DA cycloadditions for 2-thioph-e and 2-BT-e in gas phase and o-DCB respectively are shown in Figure 17 and Figure 18. I have not been able to identify the second transition state in the stepwise mechanism. This transition state is typically very difficult to locate on the potential energy surface for stepwise DA mechanisms. Having these more complete results, I can construct a clearer picture of the competing mechanisms for these two substrates. Looking at Figure 17 and Figure 18, we can see that in both cases the s-trans stepwise transition state has the lowest free energy of activation, followed by the s-cis stepwise and the s-cis concerted transition state, which has the highest barrier, although the energy differences are very small. These energy differences, within 1-2 kcal/mol, are small enough that we can say that all three transition states are energetically available, and may contribute to the overall mechanism and kinetics.

In order to get a clearer picture I attempted to correlate the computed free energies of activation with the experimental free energies of activation derived from the rates of the reactions determined in o-DCB, at an average temperature of 363 K. The computational free energies of activation at 363 K were obtained from the free energies determined at 298.15 K in o-DCB, applying a temperature correction at 363 K using the goodvibes program.

The correlation between the experimental and computed free energies of activation for all the substrates in o-DCB at 363 K is shown in Figure 19. We can see in figure 19 that both the s-cis concerted and the s-trans stepwise computed free energies of activation have a positive correlation with the experimental activation free energies. This correlation however is not very high, and for the case of the s-cis concerted mechanism it is insignificant. The correlation when taking the lower energy transition state is also positive, but very small. We can also see that the free energies for the Sulphur compounds (S-heteroarenes) are clustered closer together, but the energies for the nitrogen heteroarenes with the tosyl group replacing the hydrogen atom on nitrogen (NT-heteroarenes) have a wider range of values.

If we take these two groups of heteroarenes, the S-heteroarenes and the NT-heteroarenes, separately, we can see that the correlations are somewhat different. If we take only the data for the S-heteroarenes (Figure 21 and Figure 22), the correlation for the s-cis concerted transition states is greatly improved, and for the s-trans diradical TSs it's slightly lower, On the other hand, for the NT-heteroarenes, the correlation for the s-cis concerted TSs is low, but for the s-trans stepwise TSs, it's higher than for the S-heteroarenes.

From these results it appears that the free energies of activation of both mechanisms show a correlation with the experimental rates, which is better for the s-cis concerted TSs for the Sulphur heteroarenes, and for the s-trans stepwise TSs for the NT-heteroarene. There is no evidence for one or the other of the two competing mechanisms taking precedence under certain conditions, because taking the lower of the two computed activation free energies did not improve the correlation (Figure 20, Figure 22, and Figure 24). This once again indicates that for the set of substrates in this study, a contribution from all the mechanisms is possible. Though, it is important to note that I have not identified all of the s-cis open-shell TSs. Perhaps once the s-cis open-shell transition states are available, the picture of competing mechanisms, or a preferred mechanism for all substrates, will be clearer.

To this point, I have been studying the mechanism of the DA cycloaddition within the framework of traditional TST. It is possible that the mechanism for formation of the DA adduct can't be properly described within this framework. The shortcomings of traditional TST for describing the mechanisms of DA reactions and other similar cyclization reactions are becoming increasingly apparent[3, 36-37, 42-43]. The assumption that the ensemble of reactive trajectories can be approximated by a chemical reaction path may not be valid for more complex mechanisms.

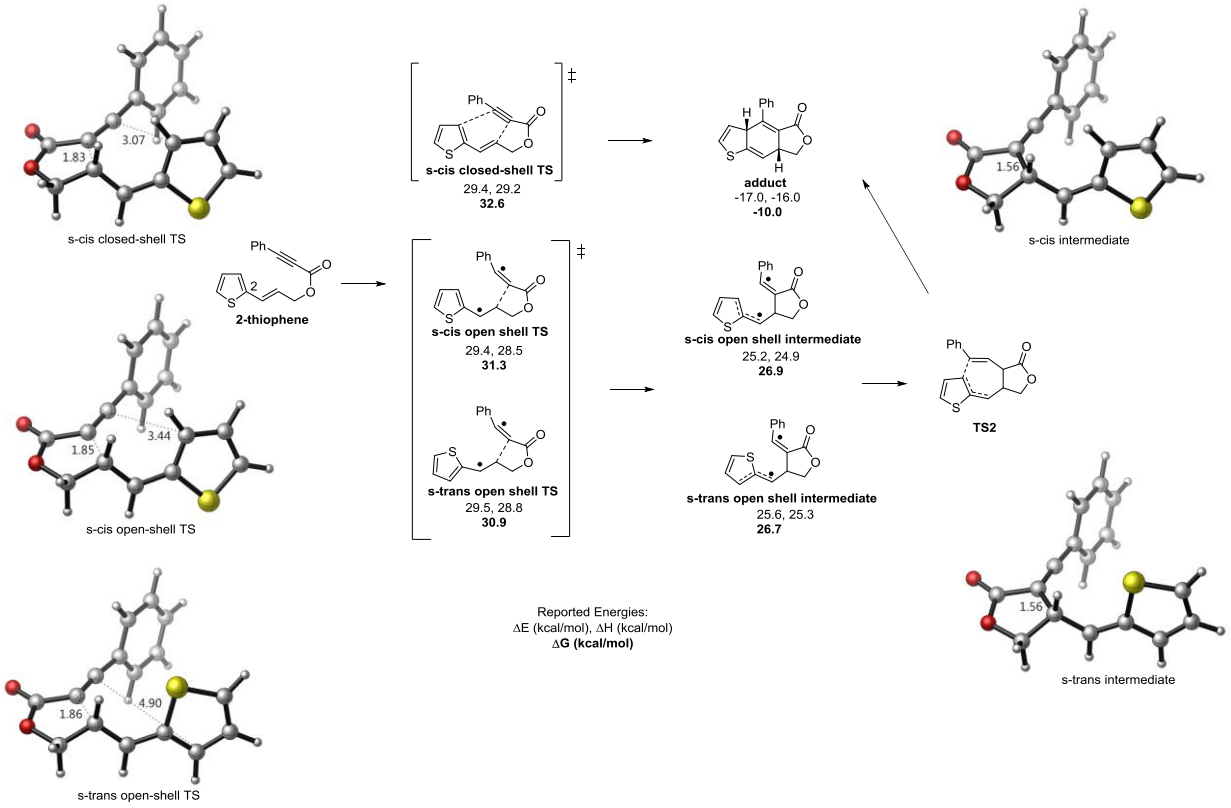

Figure 17 Proposed competing mechanisms for the formation of the Diels-Alder adduct in 2-thiophene, at the (U)B3LYP/6-311+g(d,p)//(U)b3lyp/6-31+g(d) level of theory, in the gas phase

IMDDA reactions in particular, frequently have flat potential energy surfaces with a very small energy difference between the concerted and stepwise TSs[36]. Furthermore, Singleton[42] has pointed out that the assumption that mechanisms can only be either stepwise (passing through an intermediate followed by a second energy barrier), or concerted (there is only one kinetically distinguishable step), with the possibility of competition between two mechanisms for more complicated cases, limits the kind of understanding of individual reaction mechanisms that we can achieve. Recent results indicate that when the geometry of the concerted and stepwise TSs is similar, for highly asynchronous TSs where both the cycloadduct and the intermediate are downhill from the TS, the stepwise and concerted pathway proceed through the same TS.

One way that concerted and stepwise pathways can merge is through a post transition state-bifurcation on the PES, diverging in two different directions from an initial shared transition state. In most examples of DA reactions of this

kind going, the two pathways of the bifurcation diverge in such a way that one goes directly to products, and the other passes through an intermediate and a second transition state to give the final product. Another possibility is that, instead of bifurcating from an initial TS, the stepwise and concerted pathway pass through the same region on the PES. In such a case, the concerted pathway also passes through the intermediate. The redistribution of vibrational modes, which are not always much faster than rearrangements in chemical reactions determine whether a particular trajectory will be trapped in the region of the intermediate or not[72]. In such a case, the product selectivity may not reflect the presence of an intermediate or a second kinetically distinguishable step, and a stepwise reaction may appear stereochemically concerted. So perhaps, the lack of formation of the trans-adduct is not a consequence of a concerted reaction being preferred in all cases, but of the specific dynamics of these reactions. Although the trans-adduct for these reactions had a higher relative free energy than the cis-adduct, this is only 4-5 kcal/mol (See Table 2 in the next section), and the reaction to form the trans-cycloadduct is still exothermic. Considering that the free energies of activation of the transition states are very similar in most cases, it is possible that the dynamics of these reactions is more complex, and there is contribution from all the pathways considered above.

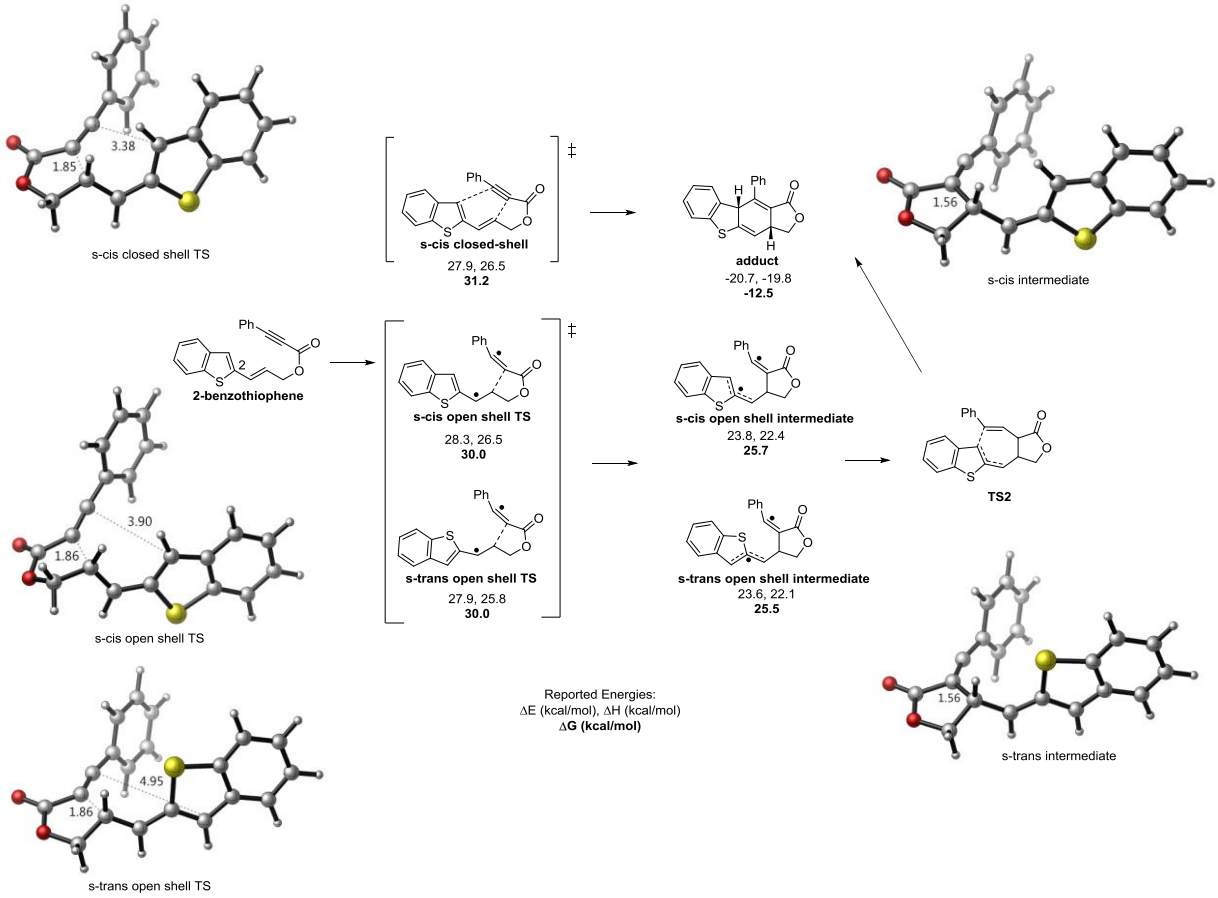

Figure 18 Proposed competing mechanisms for the formation of the Diels-Alder adduct in 2-benzothiophene, at the (U)B3LYP/6-311+g(d,p) (SMD,o-DCB)//(U)b3lyp/6-31+g(d) (SMD,o-DCB) level of theory, in the gas phase

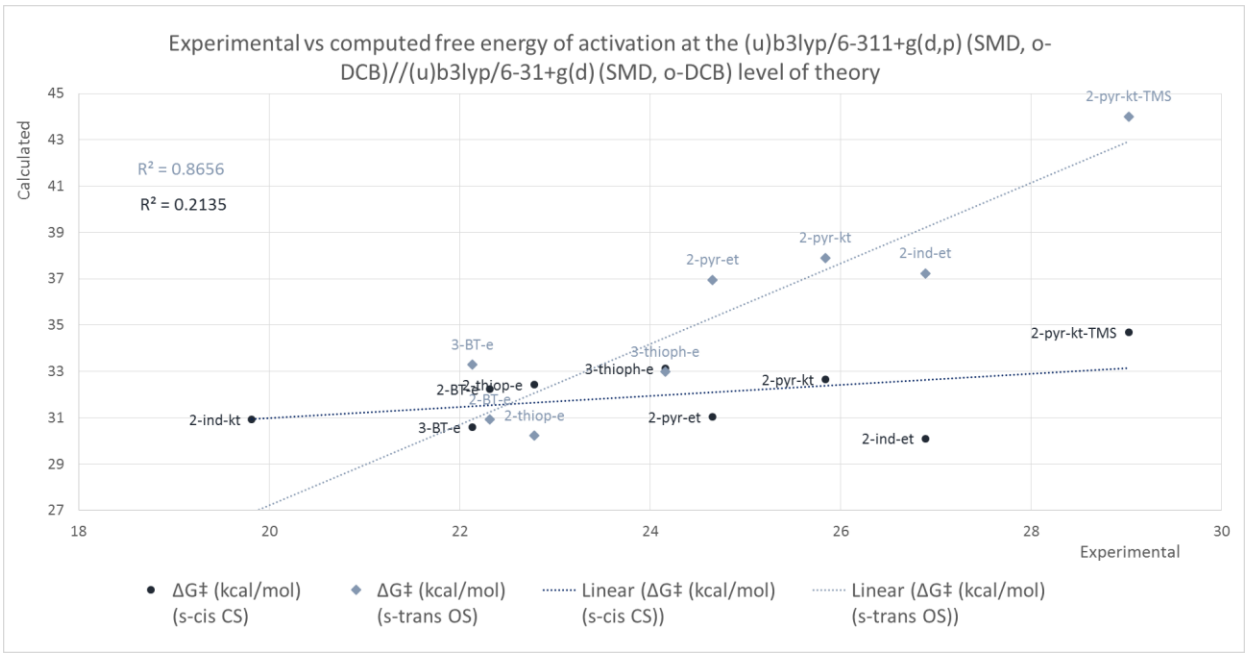

Figure 19 Correlation between the experimental and computed free energies of activation for the s-cis CS TS and s-trans OS TS for all the species

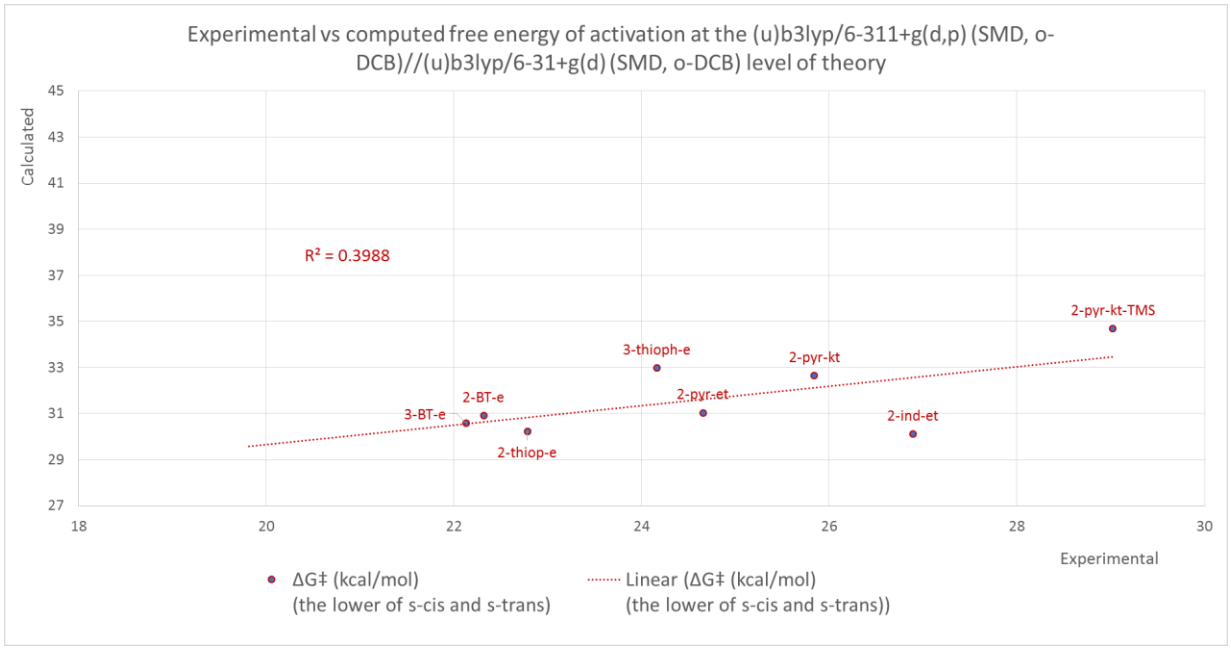

Figure 20 Correlation between the experimental and computed free energies of activation taking the lower of the s-cis CS TS and s-trans OS TS for all the species

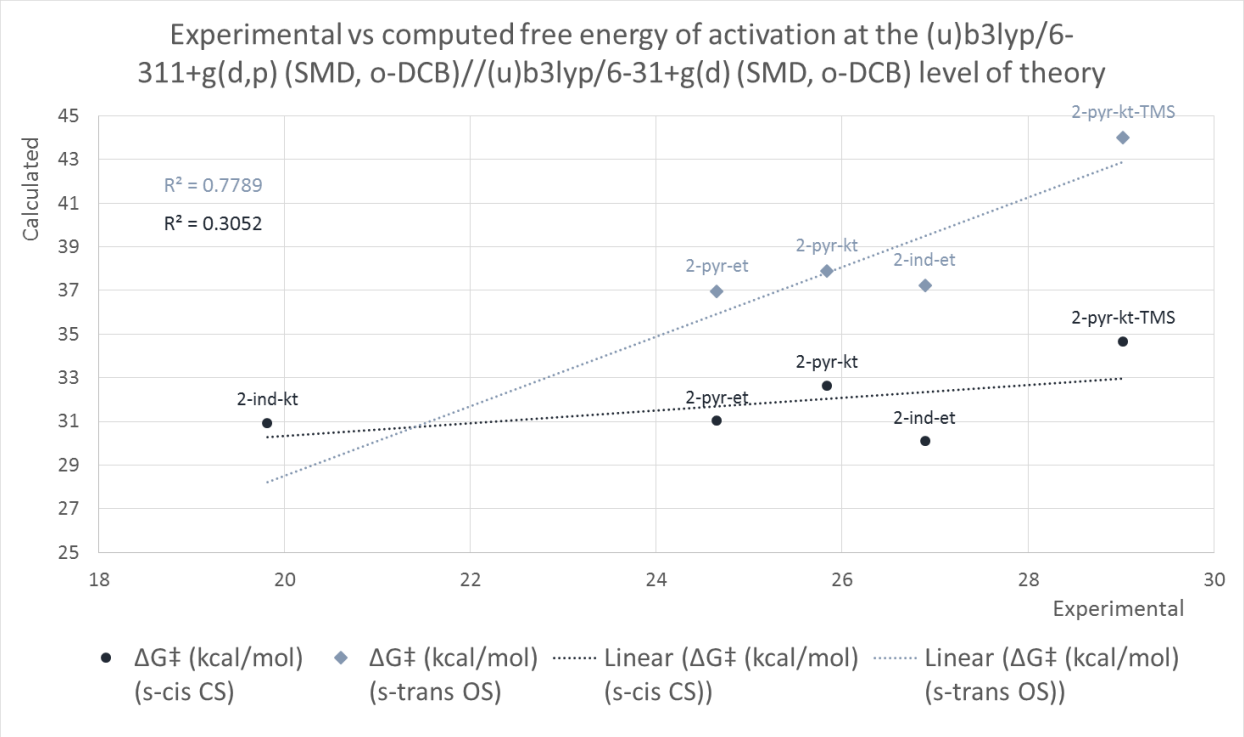

Figure 21 Correlation between the experimental and computed free energies of activation for the s-cis CS TS and s-trans OS TS for the S-heteroarenes

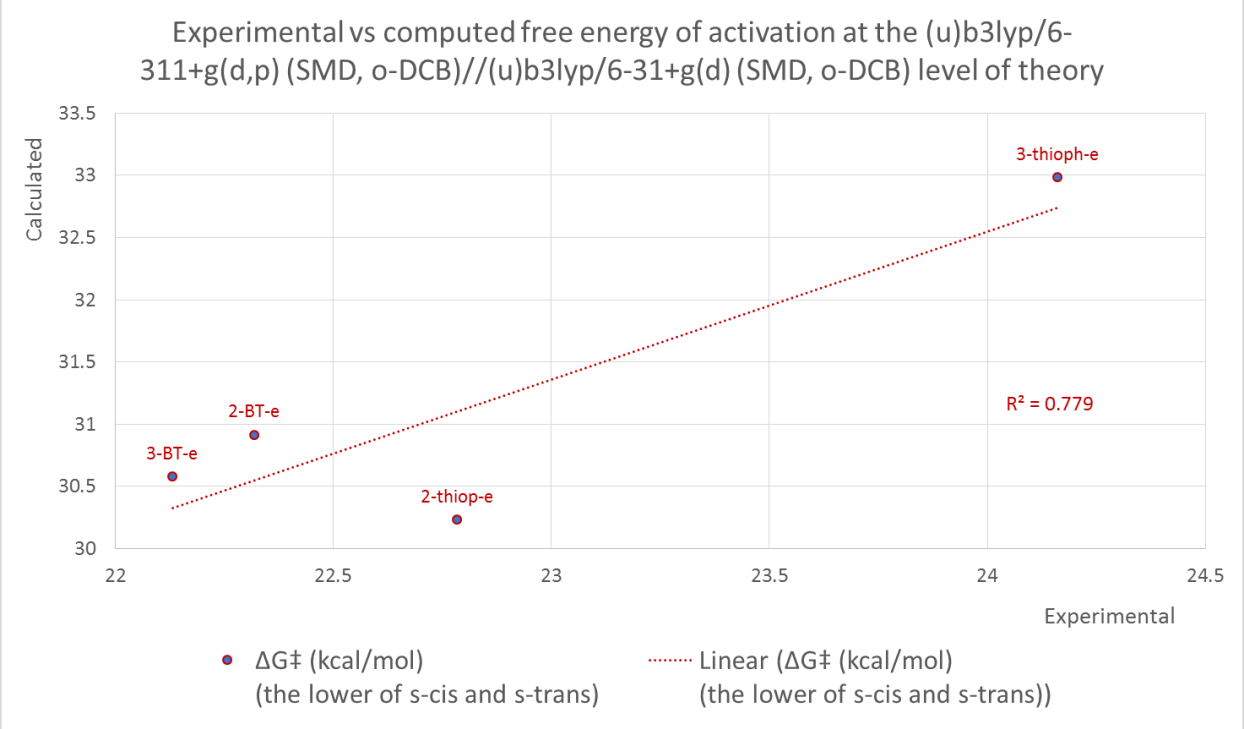

Figure 22 Correlation between the experimental and computed free energies of activation taking the lower of the s-cis CS TS and s-trans OS TS for the S-heteroarenes

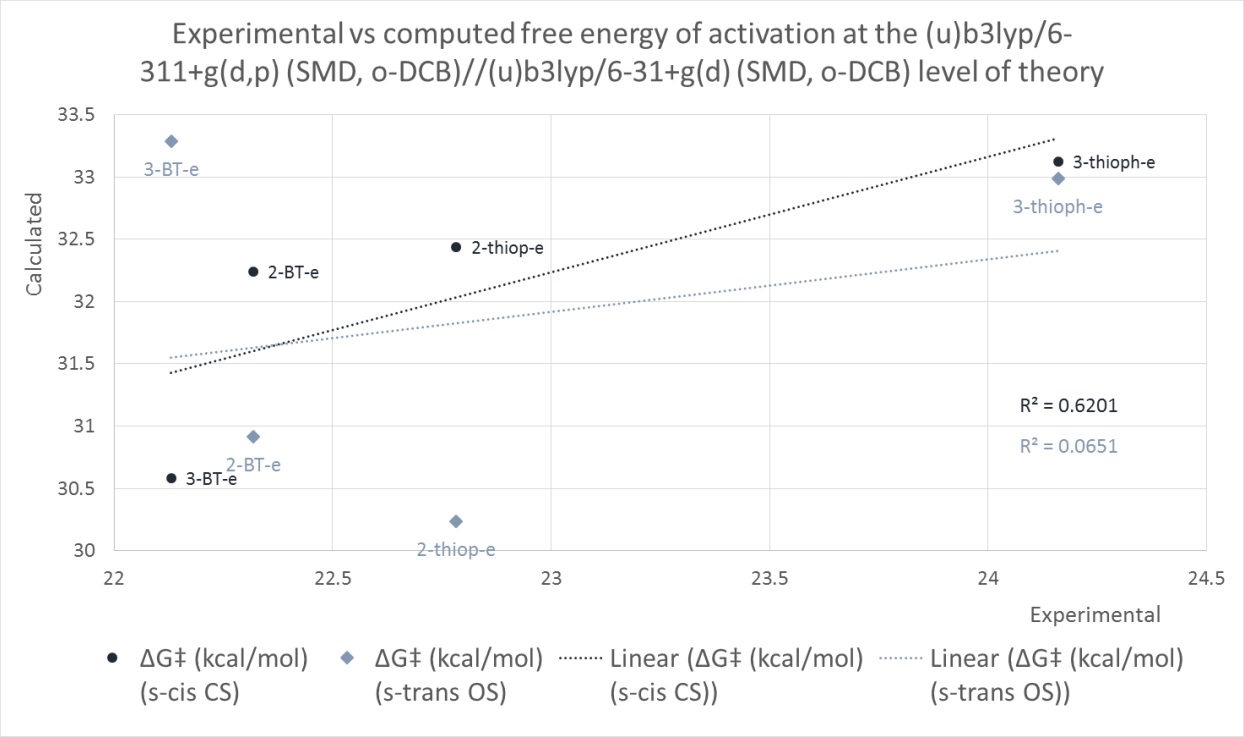

Figure 23 Correlation between the experimental and computed free energies of activation for the s-cis CS TS and s-trans OS TS for the NT-heteroarenes

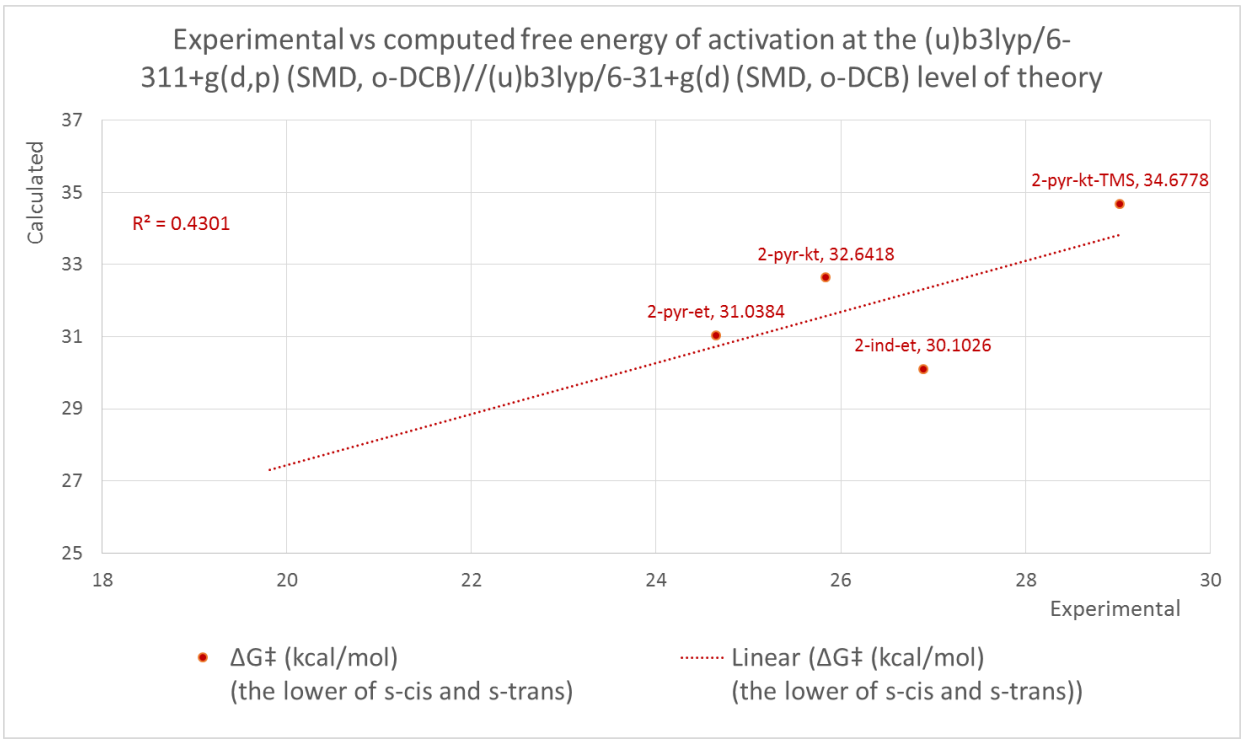

Figure 24 Correlation between the experimental and computed free energies of activation taking the lower of the s-cis CS TS and s-trans OS TS for the NT-heteroarenes

3.2 COMPUTATIONAL RESULTS FOR THE FORMATION OF THE ISOMERIZED AND THE OXIDIZED PRODUCT

The gas phase acidities (Figure 25 B) do seem to correlate with the experimental studies of the selectivity for the isomerized and oxidized product for the different substrates. The experimentally observed selectivity for the oxidized and the isomerized product agree with what we would expect based on the gas phase acidities, assuming an ionic mechanism for the formation of the isomerized product and a mechanism that does not involve protons for the formation of the oxidized product. 2-indole and 2-pyrrole have considerably lower gas phase acidities compared to 3-thiophene and 3-benzothiophene. The loss of the proton should therefore be much more energetically favorable for 2-pyrrole and 2-indole, and so they should be much more likely to undergo the ionic mechanism to form the isomerized product. This is in agreement with what is observed experimentally. 3-BT shows a much greater propensity for forming oxidized product over isomerized product, and 2-pyrrole and 2-indole show a greater propensity for the formation of isomerized product. The BDEs (Figure 11 A) do not seem to support a radical mechanism for the formation of the oxidized product. 3-BT has a very large propensity for the formation of the oxidized product, and yet it has the highest BDE value. These results suggest the formation of the oxidized product does not proceed through a radical mechanism.

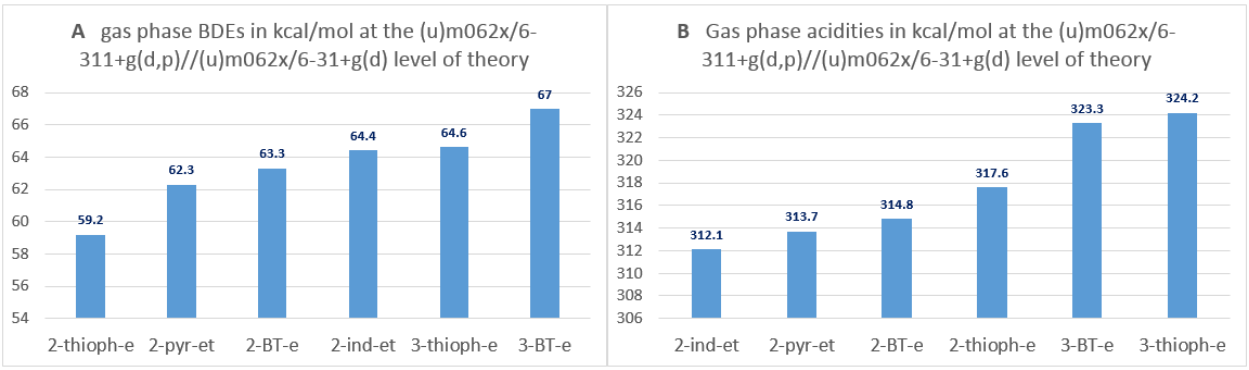

Figure 25 Gas phase acidities and BDEs

The results of the DFT calculations of the relative free energies with respect to the substrate are summarized in Table 2. Some trends in the effects of attachment position of the tether, and the effect of the benzene ring for the benzofused species are summarized in Figure 26. We can see on Figure 26 A that similarly to the transition states, there is a stabilizing effect of the benzene ring that is most noticeable for the adduct, and to some extent for the oxidized product. The trend for the isomerized product is not clear. The results in Figure 22A were obtained in gas phase, but the same trend is present in DMF and o-DCB as well. There is a similar effect for the tether attachment position, shown in Figure 26 B. Changing the tether attachment position from 2- to 3- has a stabilizing effect on the adduct, but the trend is not clear for the isomerized and the oxidized form. The solvent effect (Figures 26 C, 26 D, and 26 E) indicates a stabilization of the adduct in DMF for all substrates, and a slight destabilization of the oxidized product in o-DCB. These results are in agreement with the experimental result that the 3-benzothiophene adduct was the easiest to isolate, and the isolation was performed in DMF.

There is also a very pronounced solvent effect, particularly in DMF, for the 2-pyrrole adducts, oxidized, and isomerized products. This greater sensitivity to the solvent is accompanied by a significant change in the dipole moment for the 2-pyrole species in the DMF and o-DCB solvents with respect to the gas phase, as a consequence of different conformations being favored in different solvents. The 2-indole species also have larger dipole moments overall, and see a change in dipole moment and the lowest energy conformation in different solvents, but this effect is not as pronounced. In the other cases, the solvent effect is not clear.

The ground state free energies of the products do not correlate with the experimentally observed selectivity, confirming the assumption that the selectivity in these reactions is under kinetic control.

Table 2 Relative free energies with respect to the substrate of the DA adduct, and the isomerized, oxidized, and diene product, determined at the m062x/6-311+g(d,p) (SMD,DMF)//m062x/6-31+g(d) level of theory in DMF, o-DCB, and gas

DMF	**DA cis-Adduct**	**DA trans-Adduct**	**Isomerized Product**	**Oxidized Product**	**Diene Product**
3-thioph-e	-28.7		-47.1	-55.2	-35.6
3-BT-e	-34.3	-30.6	-48.4	-57.7	-40.8
2-thioph-e	-25.3		-47.3	-54.8	-34.3
2-BT-e	-30.3		-47.1	-55.4	-36.9
2-pyr-et	-30.9	-20.8	-49.1	-57.7	-35.5
2-ind-et	-34.7	-29.8	-47.6	-58.8	-41.5
gas phase	**Da cis-Adduct**	**DA trans-Adduct**	**Isomerized Product**	**Oxidized Product**	
3-thioph-e	-26.6		-46.1	-55.2	
3-BT-e	-32	-28.9	-47.4	-57.4	
2-thioph-e	-23.4		-46.1	-54.4	
2-BT-e	-28.7		-45.9	-55.6	
2-pyr-et	-25.6	-16.8	-45.1	-55.5	
2-ind-et	-32.7922	-27.7	-46.7	-58.5	
o-DCB	**DA cis-Adduct**	**DA trans-Adduct**	**Isomerized Product**	**Oxidized Product**	**Diene Product**
3-thioph-e	-27.6		-46.3	-54.8	-34.5
3-BT-e	-32.9	-29.2	-47.2	-58.0	-39.4
2-thioph-e	-23.8		-45.9	-53.8	-33.0
2-BT-e	-28.3		-45	-53.8	-35.0
2-pyr-et	-26.75	-17.7	-45.9	-54.70	-33.0
2-ind-et	-32.3	-26.9	-46.4	-57.3	-39.4

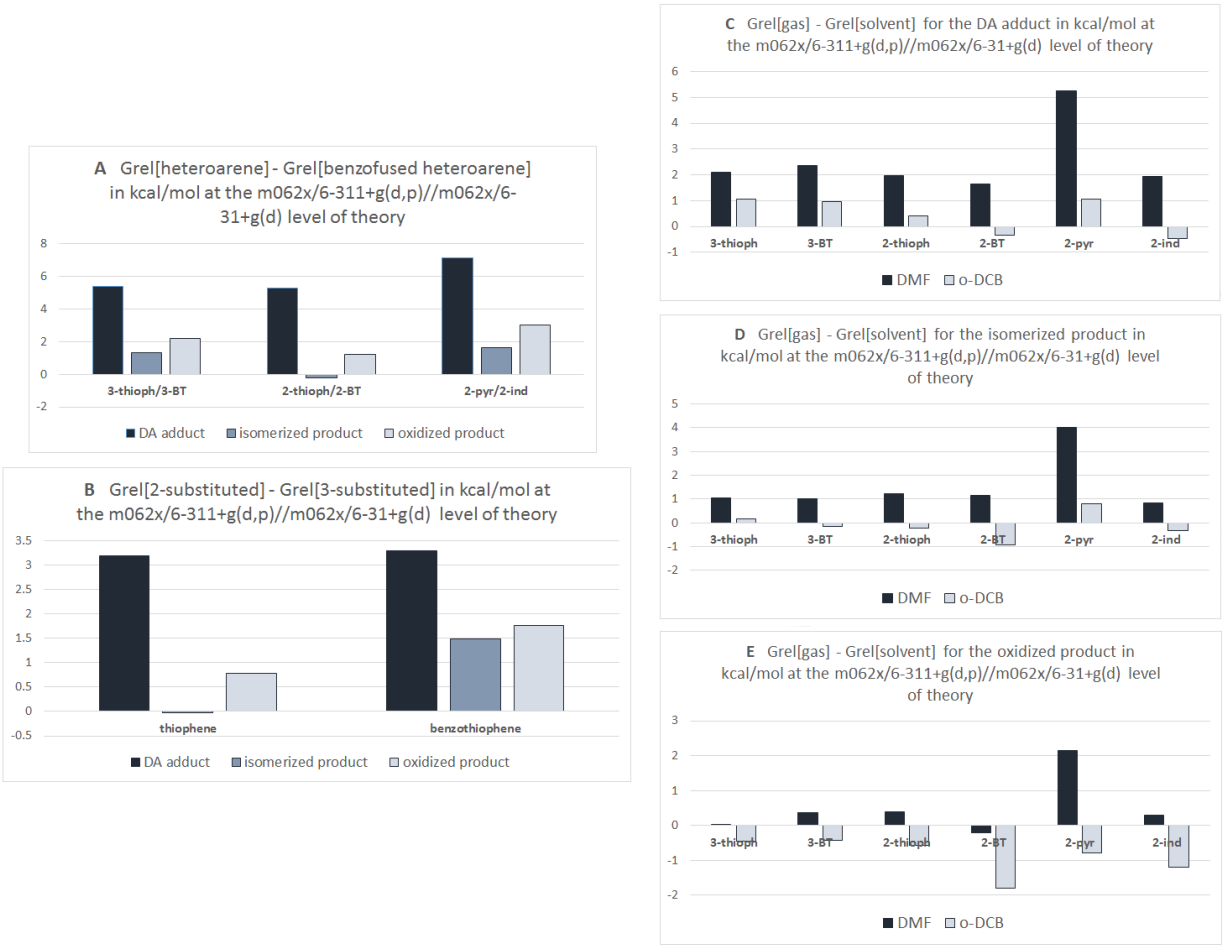

Figure 26 Analysis of the relative free energies with respect to the substrate of the DA adduct, and the isomerized, oxidized, and diene product, determined at the m062x/6-311+g(d,p) (SMD,DMF)//m062x/6-31+g(d) level of theory in DMF, o-DCB, and gas

4.0 CONCLUSION

From all this, it is clear that the IMDDA reaction of ene-yne substituted heteroarenes is a very mechanistically complex system for study due to contributions from the competing concerted and stepwise pathways in the DA step and multiple isomerization and oxidation products formed after the initial DA step. For the DA cycloaddition step, the s-cis concerted, s-cis stepwise, and s-trans stepwise transition states have similar geometries and activation free energies. Because of this, all three pathways are energetically available and can contribute to the overall reaction mechanism. There are a few interesting trends, particularly that for the 3-substituted species that do not contain a sterically prohibitive group on the heteroatom, like for example the tosy group in the nitrogen heteroarenes, the s-cis concerted mechanism is preferred, especially for the benzofused heteroarenes. It appears that the trend is reversed for the 2-substituted species, for which a stepwise s-trans mechanism is preferred, irrespective of whether the heteroarene diene contains an additional benzene ring or not. This is not a consequence of variations in aromaticity of the heteroarene with the position of substitution.

The BDE and acidity calculations support the ionic mechanism for the formation of the isomerized product. The relative free energies of the substrates indicate that the selectivity for the final product is not under thermodynamic control. The analysis of this data indicates that the 3-substituted benzofused adducts are the easiest to isolate, and that polar solvents have an additional stabilizing effect.

APPENDIX A

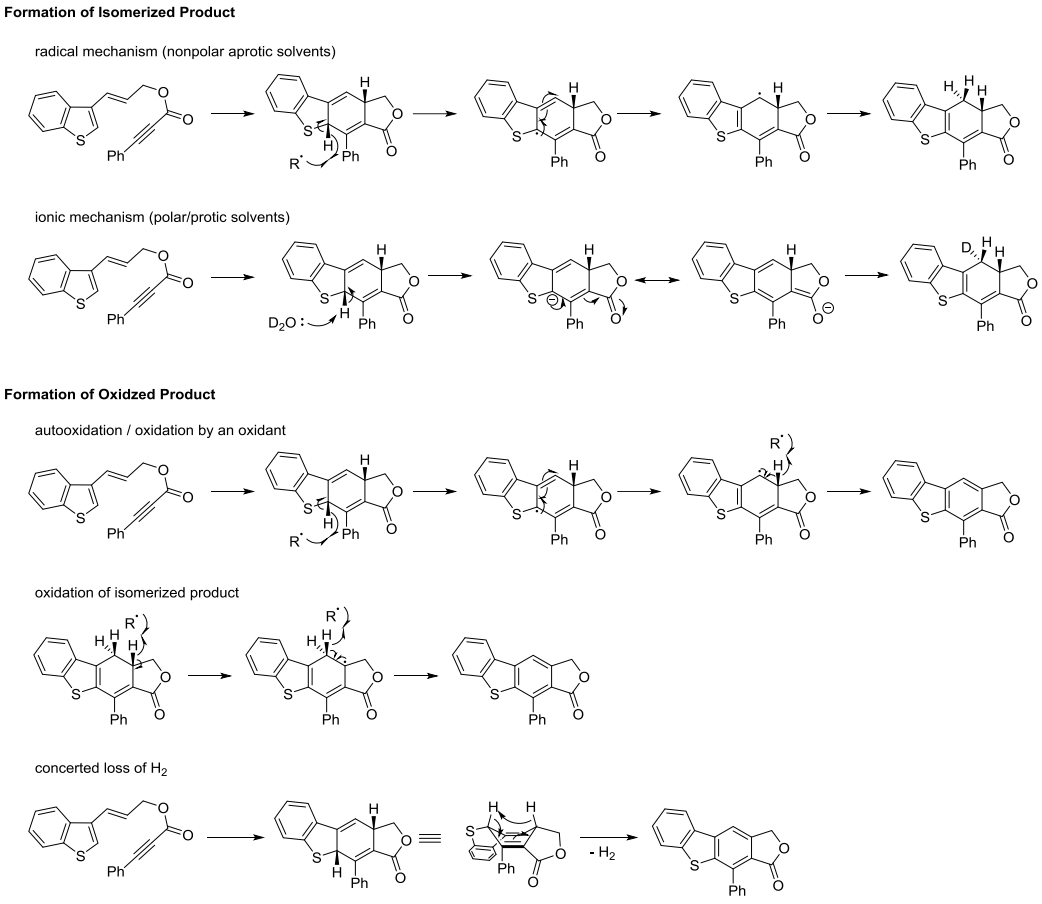

Figure A 1 Proposed mechanisms for the formation of oxidized and isomerized product[b]

APPENDIX B

Table B 1 Computed free energies of activation for the open shell and closed shell transition states of the substrates, using different functionals and solvents. The calcuations were done at the (U)M062X/6-311+g(d,p) //(U)M062X/6-31+g(d) and (U)B3LYP/6-311+g(d,p) //(U)B3LYP/6-31+g(d) levels of theory at the standard temperature in Gaussian, 273.15 K.

Functional-Solvent	$G^{‡}$ (DA-s-cis) kcal/mol	$G^{‡}$ (diradical-s-cis) kcal/mol	$G^{‡}$ (diradical-s-trans) kcal/mol
3-BT-e			
b3lyp-DMF	28.5		31.6
b3lyp-gas	31.1		34.2
b3lyp-o-DCB	29.8		32.7
m062x-DMF	26.0		32.1
m062x-gas	27.2		34.4
m062x-o-DCB	27.5		34.2
2-BT-e			
b3lyp-DMF	29.9		28.7
b3lyp-gas	32.2		30.9
b3lyp-o-DCB	31.2	30.0	30.0
m062x-DMF	25.4		
m062x-gas	26.7		
m062x-o-DCB	27.7		
3-thioph-e			
b3lyp-DMF	30.5		30.9
b3lyp-gas	33.4		33.1
b3lyp-o-DCB	32.3		32.4
m062x-DMF	28.1		37.4
m062x-gas	29.6		33.2
m062x-o-DCB	29.1		32.5
2-thioph-e			
b3lyp-DMF	30.2	29.2	28.7
b3lyp-gas	32.6	31.3	30.9
b3lyp-o-DCB	31.7		29.7
m062x-DMF	27.8		
m062x-gas	29.6		
m062x-o-DCB	29.3		
3-ind-e			
b3lyp-gas	30.4		33.1
2-ind-e			

[b] This figure was created by Ashley Bober and Joseph Winkelbauer, and presented in a meeting on the research project. I have included it here because it is relevant for the discussion.

b3lyp-DMF		28.6	
b3lyp-gas	32.4		31.1
b3lyp-o-DCB	31.4	29.8	29.4
3-pyr-e			
b3lyp-gas	32.5		32.7
2-pyr-e			
b3lyp-gas	32.8	31.3	
2-ind-et			
b3lyp-DMF	28.2		34.6
b3lyp-gas	31.3		38.2
b3lyp-o-DCB	29.2		36.3
m062x-DMF	25.4		33.4
m062x-gas	26.4		36.9
m062x-o-DCB	27.3		36.3
2-pyr-et			
b3lyp-DMF	28.5		34.2
b3lyp-gas	31.4	30.2	37.2
b3lyp-o-DCB	30.2		36.2
m062x-DMF	28.6		32.8
m062x-gas	28.9		37.0
m062x-o-DCB	31.5		35.6
2-ind-kt			
b3lyp-gas	30.4		39.5
b3lyp-o-DCB	30.2		
2-pyr-kt			
b3lyp-gas	31.3		37.8
b3lyp-o-DCB	31.7		37.3
2-pyr-kt-TMS			
b3lyp-gas	33.8		43.0
b3lyp-o-DCB	33.8		43.2

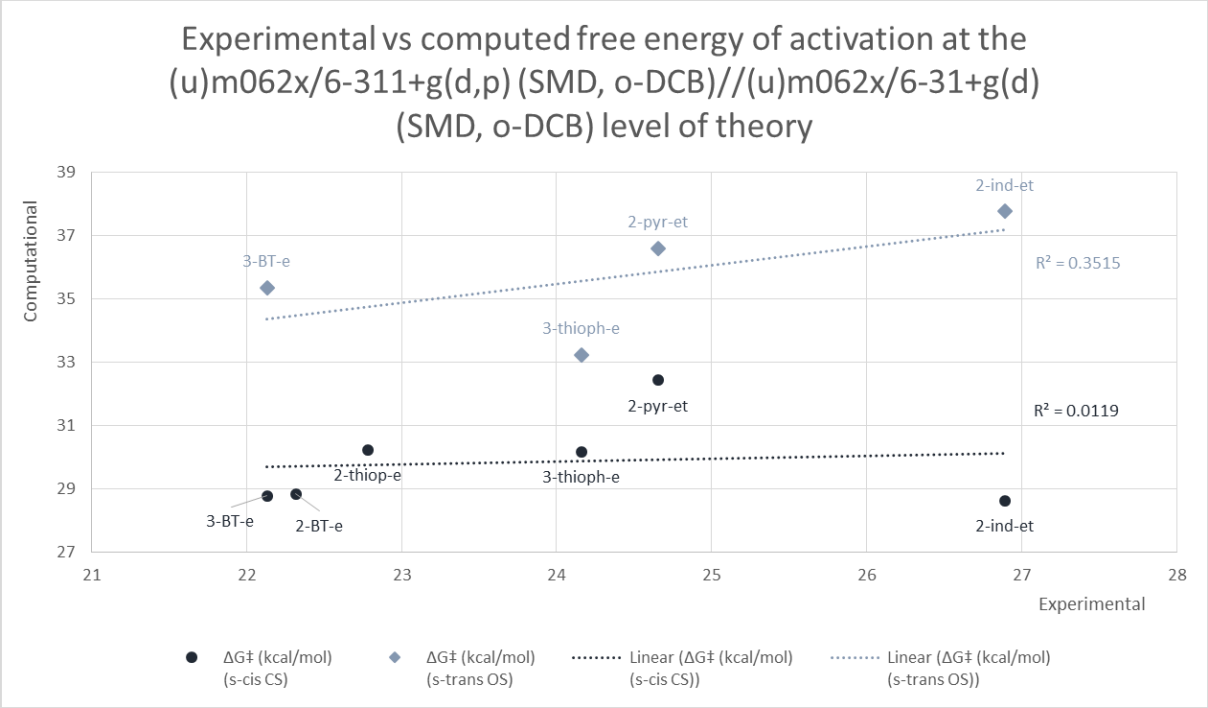

Figure B 1 Result of the correlation between the computed and experimental free energies of activation at the (U)M062X/6-311+g(d,p) (SMD,o-DCB)//(U)M062X/6-31+g(d) (SMD,o-DCB) level of theory. I have included this figure primarily, to illustrate the very poor performance of the M062X functional.

REFERENCES

1. Bober, A. E.; Proto, J. T.; Brummond, K. M., Intramolecular Didehydro-Diels–Alder Reaction for the Synthesis of Benzo- and Dihydrobenzo-Fused Heterocycles. Org. Lett. 2017, 19 (7), 1500-1503.

2. Lima, H. M.; Sivappa, R.; Yousufuddin, M.; Lovely, C. J., Total Synthesis of 7′-Desmethylkealiiquinone. Org. Lett. 2012, 14 (9), 2274-2277.

3. Rana, A.; Paul, I.; Schmittel, M., Dynamic effects in the didehydro-Diels-Alder (DDDA) reaction of enyne-ketoenes: 50% stepwise bond formation in spite of concerted transition state. J. Phys. Org. Chem. 2017, 30 (9), e3732.

4. Brummond, K. M.; Kocsis, L. S., Intramolecular Didehydro-Diels–Alder Reaction and Its Impact on the Structure–Function Properties of Environmentally Sensitive Fluorophores. Acc. Chem. Res. 2015, 48 (8), 2320-2329.

5. Kocsis, L. S.; Kagalwala, H. N.; Mutto, S.; Godugu, B.; Bernhard, S.; Tantillo, D. J.; Brummond, K. M., Mechanistic Insight into the Dehydro-Diels–Alder Reaction of Styrene–Ynes. J. Org. Chem. 2015, 80 (23), 11686-11698.

6. Hoye, T. R.; Baire, B.; Niu, D.; Willoughby, P. H.; Woods, B. P., The hexadehydro-Diels–Alder reaction. Nature 2012, 490 (7419), 208-212.

7. Wang, T.; Niu, D.; Hoye, T. R., The Hexadehydro-Diels–Alder Cycloisomerization Reaction Proceeds by a Stepwise Mechanism. J. Am. Chem. Soc. 2016, 138 (25), 7832-7835.

8. Rodríguez, D.; Navarro, A.; Castedo, L.; Domínguez, D.; Saá, C., Intramolecular [4 + 2] Cycloaddition Reactions of Diarylacetylenes: Synthesis of Benzo[b]fluorene Derivatives via Cyclic Allenes. Org. Lett. 2000, 2 (11), 1497-1500.

9. Diels, O.; Alder, K., Synthesen in der hydroaromatischen Reihe. Justus Liebigs Ann. Chem. 1928, 460 (1), 98-122.

10. Norton, J. A., The Diels-Alder Diene Synthesis. Chem. Rev. 1942, 31 (2), 319-523.

11. Martin, J. G.; Hill, R. K., Stereochemistry of the Diels-Alder Reaction. Chem. Rev. 1961, 61 (6), 537-562.

12. Nandivada, H.; Jiang, X.; Lahann, J., Click Chemistry: Versatility and Control in the Hands of Materials Scientists. Adv. Mat. 2007, 19 (17), 2197-2208.

13. Franc, G.; Kakkar, A. K., Diels–Alder "Click" Chemistry in Designing Dendritic Macromolecules. Chem.: Eur. J. 2009, 15 (23), 5630-5639.

14. Tasdelen, M. A., Diels–Alder "click" reactions: recent applications in polymer and material science. Polym. Chem. 2011, 2 (10), 2133-2145.

15. Woodward, R. B.; Hoffmann, R., The Conservation of Orbital Symmetry. Angew. Chem. Int. Ed. Engl. 1969, 8 (11), 781-853.

16. Hoffmann, R.; Woodward, R. B., Selection Rules for Concerted Cycloaddition Reactions. J. Am. Chem. Soc. 1965, 87 (9), 2046-2048.

17. Fukui, K., Molecular Orbitals. In Theory of Orientation and Stereoselection, Fukui, K., Ed. Springer Berlin Heidelberg: Berlin, Heidelberg, 1975; pp 1-7.

18. Fukui, K., Recognition of stereochemical paths by orbital interaction. Acc. Chem. Res. 1971, 4 (2), 57-64.

19. Zimmerman, H. E., Moebius-Hueckel concept in organic chemistry. Application of organic molecules and reactions. Acc. Chem. Res. 1971, 4 (8), 272-280.

20. Houk, K. N.; Liu, F.; Yang, Y.-F.; Hong, X., The Distortion/Interaction Model for Analysis of Activation Energies of Organic Reactions. In Applied Theoretical Organic Chemistry, WORLD SCIENTIFIC (EUROPE): 2017; pp 371-402.

21. Hare, S. R.; Tantillo, D. J., Post-transition state bifurcations gain momentum – current state of the field. Pure and Applied Chemistry 2017, 89 (6), 679-698.

22. Ess, D. H.; Wheeler, S. E.; Iafe, R. G.; Xu, L.; Çelebi-Ölçüm, N.; Houk, K. N., Bifurcations on Potential Energy Surfaces of Organic Reactions. Angew. Chem. Int. Ed. Engl. 2008, 47 (40), 7592-7601.

23. Black, K.; Liu, P.; Xu, L.; Doubleday, C.; Houk, K. N., Dynamics, transition states, and timing of bond formation in Diels–Alder reactions. PNAS 2012, 109 (32), 12860-12865.

24. Bradley, A. Z.; Kociolek, M. G.; Johnson, R. P., Conformational Selectivity in the Diels−Alder Cycloaddition: Predictions for Reactions of s-trans-1,3-Butadiene. J. Org. Chem. 2000, 65 (21), 7134-7138.

25. Houk, K. N.; Lin, Y. T.; Brown, F. K., Evidence for the concerted mechanism of the Diels-Alder reaction of butadiene with ethylene. J. Am. Chem. Soc. 1986, 108 (3), 554-556.

26. Sakai, S., Theoretical Analysis of Concerted and Stepwise Mechanisms of Diels−Alder Reaction between Butadiene and Ethylene. J. Phys. Chem. A 2000, 104 (5), 922-927.

27. Goldstein, E.; Beno, B.; Houk, K. N., Density Functional Theory Prediction of the Relative Energies and Isotope Effects for the Concerted and Stepwise Mechanisms of the Diels−Alder Reaction of Butadiene and Ethylene. J. Am. Chem. Soc. 1996, 118 (25), 6036-6043.

28. Doering, W. v. E.; Franck-Neumann, M.; Hasselmann, D.; Kaye, R. L., Mechanism of a Diels-Alder reaction. Butadiene and its dimers. J. Am. Chem. Soc. 1972, 94 (11), 3833-3844.

29. Saunders, M.; Jiménez-Vázquez, H. A., Stochastic searches for lactone and cycloalkene conformers. J. Comput. Chem. 1993, 14 (3), 330-348.

30. Johnson, R. P.; DiRico, K. J., Ab Initio Conformational Analysis of trans-Cyclohexene. J. Org. Chem. 1995, 60 (4), 1074-1076.

31. Pham, H. V.; Houk, K. N., Diels–Alder Reactions of Allene with Benzene and Butadiene: Concerted, Stepwise, and Ambimodal Transition States. J. Org. Chem. 2014, 79 (19), 8968-8976.

32. Tian, J.; Houk, K. N.; Klärner, F. G., Substituent Effect on Stereospecificity and Energy of Concert of the Retro-Diels−Alder Reaction of Isopropylidenenorbornene. J. Phys. Chem. A 1998, 102 (39), 7662-7667.

33. Sakai, S.; Okumura, T., Theoretical studies on the substituent effects for concerted and stepwise mechanisms of the Diels–Alder reaction between butadiene and ethylene. J. Mol. Struct.: THEOCHEM 2004, 685 (1), 89-95.

34. Wessig, P.; Müller, G., The Dehydro-Diels−Alder Reaction. Chem. Rev. 2008, 108 (6), 2051-2063.

35. Johnson, R. P., Dehydropericyclic routes to reactive intermediates. J. Phys. Org. Chem. 2010, 23 (4), 283-292.

36. Ajaz, A.; Bradley, A. Z.; Burrell, R. C.; Li, W. H. H.; Daoust, K. J.; Bovee, L. B.; DiRico, K. J.; Johnson, R. P., Concerted vs Stepwise Mechanisms in Dehydro-Diels–Alder Reactions. J. Org. Chem. 2011, 76 (22), 9320-9328.

37. Marell, D. J.; Furan, L. R.; Woods, B. P.; Lei, X.; Bendelsmith, A. J.; Cramer, C. J.; Hoye, T. R.; Kuwata, K. T., Mechanism of the Intramolecular Hexadehydro-Diels–Alder Reaction. J. Org. Chem. 2015, 80 (23), 11744-11754.

38. Wang, T.; Hoye, T. R., Hexadehydro-Diels–Alder (HDDA)-Enabled Carbazolyne Chemistry: Single Step, de Novo Construction of the Pyranocarbazole Core of Alkaloids of the Murraya koenigii (Curry Tree) Family. J. Am. Chem. Soc. 2016, 138 (42), 13870-13873.

39. Ananikov, V. P., Ab initio study of the mechanisms of intermolecular and intramolecular [4 + 2] cycloaddition reactions of conjugated enynes. J. Phys. Org. Chem. 2001, 14 (2), 109-121.

40. Ozawa, T.; Kurahashi, T.; Matsubara, S., Dehydrogenative Diels–Alder Reaction. Org. Lett. 2011, 13 (19), 5390-5393.

41. Stolle, W. A. W.; Frissen, A. E.; Marcelis, A. T. M.; Van der Plas, H. C., Intramolecular Diels-Alder reactions of pyrimidines and a computational study toward their structure and reactivity. J. Org. Chem. 1992, 57 (11), 3000-3007.

42. Bekele, T.; Christian, C. F.; Lipton, M. A.; Singleton, D. A., "Concerted" Transition State, Stepwise Mechanism. Dynamics Effects in C2-C6 Enyne Allene Cyclizations. J. Am. Chem. Soc. 2005, 127 (25), 9216-9223.

43. Gonzalez-James, O. M.; Kwan, E. E.; Singleton, D. A., Entropic Intermediates and Hidden Rate-Limiting Steps in Seemingly Concerted Cycloadditions. Observation, Prediction, and Origin of an Isotope Effect on Recrossing. J. Am. Chem. Soc. 2012, 134 (4), 1914-1917.

44. Frisch, M. J.; Trucks, G. W.; Schlegel, H. B.; Scuseria, G. E.; Robb, M. A.; Cheeseman, J. R.; Scalmani, G.; Barone, V.; Petersson, G. A.; Nakatsuji, H.; Li, X.; Caricato, M.; Marenich, A.; Bloino, J.; Janesko, B. G.; Gomperts, R.; Mennucci, B.; Hratchian, H. P.; Ortiz, J. V.; Izmaylov, A. F.; Sonnenberg, J. L.; Williams-Young, D.; Ding, F.; Lipparini, F.; Egidi, F.; Goings, J.; Peng, B.; Petrone, A.; Henderson, T.; Ranasinghe, D.; Zakrzewski, V. G.; Gao, J.; Rega, N.; Zheng, G.; Liang, W.; Hada, M.; Ehara, M.; Toyota, K.; Fukuda, R.; Hasegawa, J.; Ishida, M.; Nakajima, T.; Honda, Y.; Kitao, O.; Nakai, H.; Vreven, T.; Throssell, K.; J. A. Montgomery, J.; Peralta, J. E.; Ogliaro, F.; Bearpark, M. J.; Heyd, J. J.; Brothers, E. N.; Kudin, K. N.; Staroverov, V. N.; Keith, T. A.; Kobayashi, R.; Normand, J.; Raghavachari, K.; Rendell, A. P.; Burant, J. C.; Iyengar, S. S.; Tomasi, J.; Cossi, M.; Millam, J. M.; Klene, M.; Adamo, C.; Cammi, R.; Ochterski, J. W.; Martin, R. L.; Morokuma, K.; Farkas, O.; Foresman, J. B.; Fox, D. J. Gaussian 16, Revision A.03; Gaussian Inc.: Wallingford CT, 2016.

45. Bachrach, S. M., In Computational Organic Chemistry, 2 edition ed.; Wiley: Hoboken, New Jersey, 2014; p 199.

46. Becke, A. D., Density-functional thermochemistry. III. The role of exact exchange. J. Chem. Phys. 1993, 98 (7), 5648-5652.

47. Becke, A. D., A new mixing of Hartree–Fock and local density-functional theories. J. Chem. Phys. 1993, 98 (2), 1372-1377.

48. Lee, C.; Yang, W.; Parr, R. G., Development of the Colle-Salvetti correlation-energy formula into a functional of the electron density. Phys. Rev. B 1988, 37 (2), 785-789.

49. Stephens, P. J.; Devlin, F. J.; Chabalowski, C. F.; Frisch, M. J., Ab Initio Calculation of Vibrational Absorption and Circular Dichroism Spectra Using Density Functional Force Fields. J. Phys. Chem. 1994, 98 (45), 11623-11627.

50. Guner, V.; Khuong, K. S.; Leach, A. G.; Lee, P. S.; Bartberger, M. D.; Houk, K. N., A Standard Set of Pericyclic Reactions of Hydrocarbons for the Benchmarking of Computational Methods: The Performance of ab Initio, Density

Functional, CASSCF, CASPT2, and CBS-QB3 Methods for the Prediction of Activation Barriers, Reaction Energetics, and Transition State Geometries. J. Phys. Chem. A 2003, 107 (51), 11445-11459.

51. Jursic, B.; Zdravkovski, Z., DFT study of the Diels–Alder reactions between ethylene with buta-1,3-diene and cyclopentadiene. J. Chem. Soc., Perkin Trans. 2 1995, 0 (6), 1223-1226.

52. Zhao, Y.; Truhlar, D. G., The M06 suite of density functionals for main group thermochemistry, thermochemical kinetics, noncovalent interactions, excited states, and transition elements: two new functionals and systematic testing of four M06-class functionals and 12 other functionals. Theor. Chem. Acc. 2008, 120 (1), 215-241.

53. Frisch, M. J.; Pople, J. A.; Binkley, J. S., Self-consistent molecular orbital methods 25. Supplementary functions for Gaussian basis sets. J. Chem. Phys. 1984, 80 (7), 3265-3269.

54. Hehre, W. J.; Ditchfield, R.; Pople, J. A., Self—Consistent Molecular Orbital Methods. XII. Further Extensions of Gaussian—Type Basis Sets for Use in Molecular Orbital Studies of Organic Molecules. J. Chem. Phys. 1972, 56 (5), 2257-2261.

55. Zhao, Y.; Truhlar, D. G., Applications and validations of the Minnesota density functionals. Chem. Phys. Lett. 2011, 502 (1), 1-13.

56. Valero, R.; Costa, R.; de P. R. Moreira, I.; Truhlar, D. G.; Illas, F., Performance of the M06 family of exchange-correlation functionals for predicting magnetic coupling in organic and inorganic molecules. J. Chem. Phys. 2008, 128 (11), 114103.

57. James, N. C.; Um, J. M.; Padias, A. B.; Hall, H. K.; Houk, K. N., Computational Investigation of the Competition between the Concerted Diels–Alder Reaction and Formation of Diradicals in Reactions of Acrylonitrile with Nonpolar Dienes. J. Org. Chem. 2013, 78 (13), 6582-6592.

58. Xu, Y.; Qi, X.; Zheng, P.; Berti, C. C.; Liu, P.; Dong, G., Deacylative transformations of ketones via aromatization-promoted C–C bond activation. Nature 2019, 567 (7748), 373.

59. Pieniazek, S. N.; Clemente, F. R.; Houk, K. N., Sources of Error in DFT Computations of C□C Bond Formation Thermochemistries: π→σ Transformations and Error Cancellation by DFT Methods. Angew. Chem. Int. Ed. Engl. 2008, 47 (40), 7746-7749.

60. Marenich, A. V.; Cramer, C. J.; Truhlar, D. G., Universal Solvation Model Based on Solute Electron Density and on a Continuum Model of the Solvent Defined by the Bulk Dielectric Constant and Atomic Surface Tensions. J. Phys. Chem. B 2009, 113 (18), 6378-6396.

61. Ribeiro, R. F.; Marenich, A. V.; Cramer, C. J.; Truhlar, D. G., Use of Solution-Phase Vibrational Frequencies in Continuum Models for the Free Energy of Solvation. J. Phys. Chem. B 2011, 115 (49), 14556-14562.

62. Grimme, S., Supramolecular Binding Thermodynamics by Dispersion-Corrected Density Functional Theory. Chem.: Eur. J. 2012, 18 (32), 9955-9964.

63. Alecu, I. M.; Zheng, J.; Zhao, Y.; Truhlar, D. G., Computational Thermochemistry: Scale Factor Databases and Scale Factors for Vibrational Frequencies Obtained from Electronic Model Chemistries. J. Chem. Theory Comput. 2010, 6 (9), 2872-2887.

64. Mammen, M.; Shakhnovich, E. I.; Deutch, J. M.; Whitesides, G. M., Estimating the Entropic Cost of Self-Assembly of Multiparticle Hydrogen-Bonded Aggregates Based on the Cyanuric Acid·Melamine Lattice. J. Org. Chem. 1998, 63 (12), 3821-3830.

65. Paton, R.; Funes-Ardoiz, I.; Rodríguez-Guerra, J. Goodvibes.

66. Legault, C. Y. CYLview, 1.0b; Université de Sherbrooke, 2009.

67. Schaftenaar, G.; Noordik, J. H., Molden: a pre- and post-processing program for molecular and electronic structures. J. Comput.-Aided Mol. Design 2000, 14, 123-134.

68. Chen, Z.; Wannere, C. S.; Corminboeuf, C.; Puchta, R.; Schleyer, P. v. R., Nucleus-Independent Chemical Shifts (NICS) as an Aromaticity Criterion. Chem. Rev. 2005, 105 (10), 3842-3888.

69. Cyrański, M. K., Energetic Aspects of Cyclic Pi-Electron Delocalization: Evaluation of the Methods of Estimating Aromatic Stabilization Energies. Chem. Rev. 2005, 105 (10), 3773-3811.

70. Fallah-Bagher-Shaidaei, H.; Wannere, C. S.; Corminboeuf, C.; Puchta, R.; Schleyer, P. v. R., Which NICS Aromaticity Index for Planar π Rings Is Best? Org. Lett. 2006, 8 (5), 863-866.

71. Schleyer, P. v. R.; Manoharan, M.; Wang, Z.-X.; Kiran, B.; Jiao, H.; Puchta, R.; van Eikema Hommes, N. J. R., Dissected Nucleus-Independent Chemical Shift Analysis of π-Aromaticity and Antiaromaticity. Org. Lett. 2001, 3 (16), 2465-2468.

72. Carpenter, B. K., Dynamic Behavior of Organic Reactive Intermediates. Angew. Chem. Int. Ed. Engl. 1998, 37 (24), 3340-3350.